

RESEARCH

Open Access



# Gut dysbiosis induces the development of mastitis through a reduction in host anti-inflammatory enzyme activity by endotoxemia

Caijun Zhao<sup>1†</sup>, Xiaoyu Hu<sup>1†</sup>, Lijuan Bao<sup>1</sup>, Keyi Wu<sup>1</sup>, Yihong Zhao<sup>1</sup>, Kaihe Xiang<sup>1</sup>, Shuang Li<sup>1</sup>, Ying Wang<sup>1</sup>, Min Qiu<sup>1</sup>, Lianjun Feng<sup>1</sup>, Xiangyue Meng<sup>2</sup>, Naisheng Zhang<sup>1</sup> and Yunhe Fu<sup>1\*</sup>

## Abstract

**Background:** Mounting experimental evidence has shown that the gut microbiota plays a significant role in the pathogenesis of mastitis, and clinical investigations have found that the occurrence of mastitis is correlated with ruminal dysbiosis. However, the underlying mechanism by which the ruminal microbiota participates in the development of mastitis remains unknown.

**Results:** In the present study, we found that cows with clinical mastitis had marked systemic inflammation, which was associated with significant ruminal dysbiosis, especially enriched *Proteobacteria* in the rumen. Ruminal microbiota transplantation from mastitis cows (M-RMT) to mice induced mastitis symptoms in recipient mice along with increased mammary proinflammatory signature activation of the TLR4-cGAS-STING-NF-κB/NLRP3 pathways. M-RMT also induced mucosal inflammation and impaired intestinal barrier integrity, leading to increased endotoxemia and systemic inflammation. Moreover, we showed that M-RMT mirrored ruminal microbiota disruption in the gut of recipient mice, as evidenced by enriched *Proteobacteria* and similar bacterial functions, which were correlated with most proinflammatory parameters and serum lipopolysaccharide (LPS) levels in mice. Recurrent low-grade LPS treatment mirrored gut dysbiosis-induced endotoxemia and caused severe mastitis in mice. Furthermore, we found that gut dysbiosis-derived LPS reduced host alkaline phosphatase activity by activating neuraminidase (Neu), which facilitates low-grade LPS exposure and *E. coli*-induced mastitis in mice. Conversely, treatment with calf intestinal alkaline phosphatase or the Neu inhibitor zanamivir alleviated low-grade LPS exposure and *E. coli*-induced mastitis in mice.

**Conclusions:** Our results suggest that ruminal dysbiosis-derived low-grade endotoxemia can cause mastitis and aggravate pathogen-induced mastitis by impairing host anti-inflammatory enzymes, which implies that regulating the ruminal or gut microbiota to prevent low-grade systemic inflammation is a potential strategy for mastitis intervention.

**Keywords:** Ruminal microbiota, Mastitis, Dysbiosis, LPS, ALP, Neu

<sup>†</sup>Caijun Zhao and Xiaoyu Hu contributed equally to this work.

\*Correspondence: fuyunhesky@sina.com

<sup>1</sup> Department of Clinical Veterinary Medicine, College of Veterinary Medicine, Jilin University, Changchun 130062, Jilin Province, China  
Full list of author information is available at the end of the article

## Introduction

Mastitis is one of the most important diseases affecting the dairy industry, as it reduces milk yield and quality and thus causes great economic losses every year worldwide [1–3]. Pathogen invasions, especially those by bacteria,



have long been at the forefront of the causes of mastitis, as evidenced by pathogenic bacteria being isolated from cows with mastitis and induced mastitis symptoms in animal models [4]. However, in some mastitis cases, no pathogenic infections are detected [5, 6], and the antibiotics are not resolving the disease and mastitis becomes chronic [7]. In addition, mastitis is commonly detected in cows with gastrointestinal diseases, such as subacute ruminal acidosis (SARA) [8–10], and its occurrence is often correlated with increased intake of a high grain diet (HGD) [8–10]. Our previous study also found that consumption of a HGD to induce SARA can increase somatic cell counts (SCC) in milk and promote mammary injury [8]. These phenomena indicate that other factors may contribute to the pathogenesis of mastitis.

Among the factors affecting host physiological function and disease outcome is the gut microbiota, a sophisticated ecosystem orchestrated by commensal microorganisms in the gut [11]. Mounting studies have revealed that the gut microbiota participates in multiple host functions, including food digestion, nutrient absorption, barrier integrity maintenance, and immune and metabolic regulation [11]. Likewise, environmental or host factors, such as dietary changes, contribute to the shaping of the gut microbiota [12]. Disturbance of the gut microbiota, a phenomenon referred to as gut dysbiosis [13], has been reported to be involved in the disease processes in humans and animals, including inflammatory bowel disease [14], metabolic syndrome [15], cancer [16], autism spectrum disorder [17], and infections [18]. Our previous results demonstrated that gut dysbiosis caused by antibiotics contributed to the initiation and development of mastitis, while fecal microbiota transplantation (FMT) from healthy mice improved mastitis outcomes in mice [19]. Moreover, supplementing mice with tryptophan ameliorated *Escherichia coli* (*E. coli*)-induced mastitis in a microbiota-dependent manner [20].

The composition and function of the ruminant intestinal microbiota are spatially specific with intestinal extension [21]. Chen et al. found that ruminal microbiota profiles in cows are similar to the colonic microbiota in mice by using ruminal microbiota transplantation (RMT) from cows to antibiotic-treated mice [22]. Ruminal inflammation caused by a HGD-induced SARA can also be detected in the colon in recipient mice by RMT [22]. These indicate that the ruminal microbiota located in the main fermentation organs of ruminants may best represent the characteristics of the gastrointestinal microbiota of dairy cows. However, whether and how the ruminal microbiota participates in the pathogenesis of mastitis remain unclear.

Although it is inconclusive how gut dysbiosis mediates disease outcomes in remote organs, gut

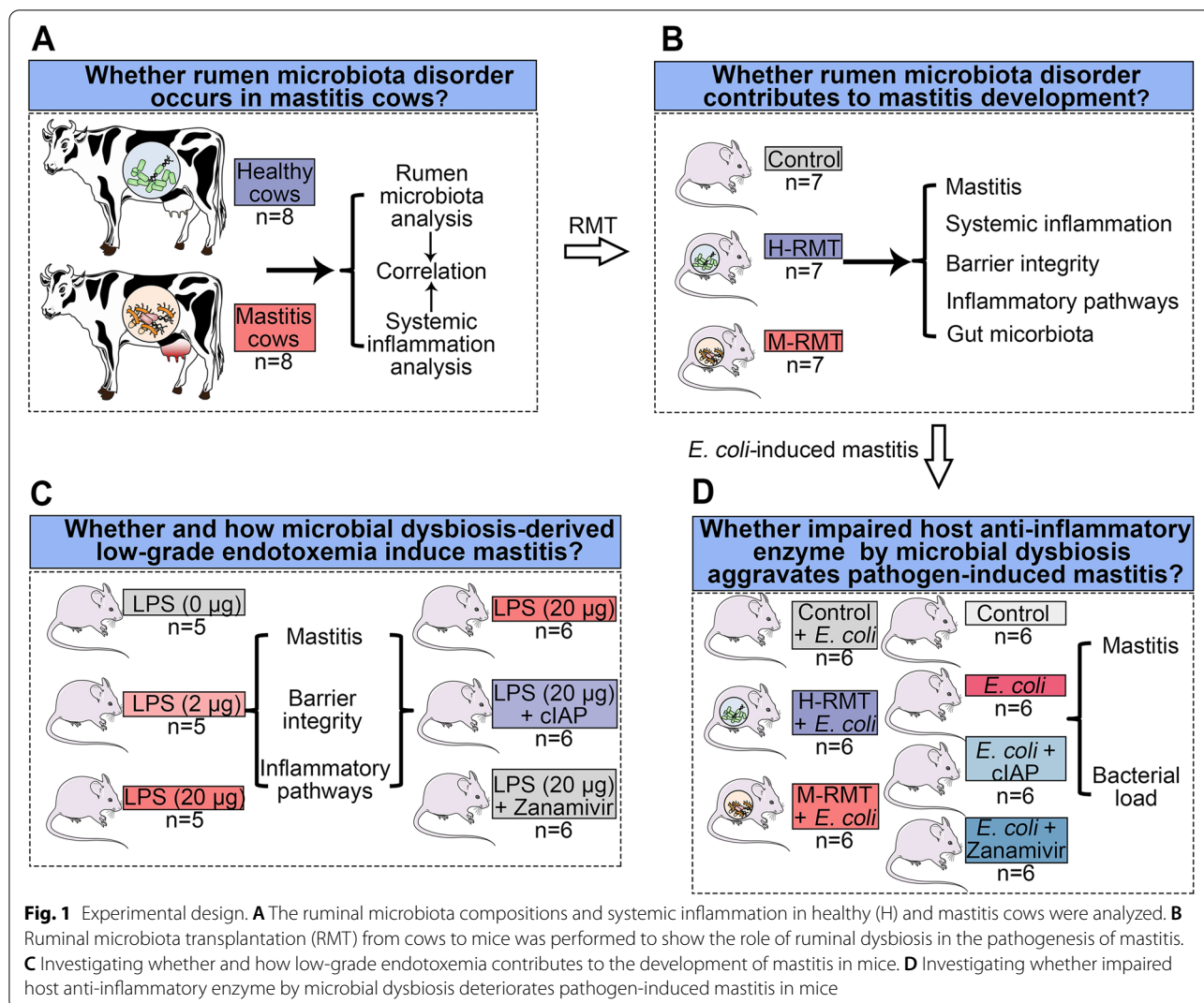
dysbiosis-induced intestinal inflammation may serve as the first step in regulating disease development [23, 24]. Studies have indicated that increased intestinal inflammation derived from gut dysbiosis can fuel microbiota disturbance in turn by growing facultative anaerobes in mice [25], particularly *Enterobacteriaceae*, by promoting an increase in intestinal oxygen content [25, 26]. Enriched *Enterobacteriaceae* further facilitate intestinal inflammation by increasing the release of bacterial toxins, such as lipopolysaccharide (LPS). These factors synergistically induce gut barrier disruption and allow harmful metabolite translocation into the blood, subsequently causing systemic inflammatory responses [23, 27, 28]. Indeed, increased LPS levels were detected in many gut dysbiosis-associated extraintestinal diseases, such as Alzheimer's disease [27, 28], obesity [29], and preeclampsia [23]. However, whether increased LPS levels derived from ruminal dysbiosis are responsible for the development of mastitis and how low-grade LPS causes mastitis have not been elucidated.

Hosts have developed complex mechanisms to degrade toxic substances, such as the alkaline phosphatase (ALP)-mediated detoxification of LPS through dephosphorylation [30, 31]. Conversely, pathogen virulence factors, including LPS, inhibit host anti-inflammatory enzyme production by reshaping host signal transduction [30–32]. Hence, we assume that ruminal dysbiosis-derived low-grade LPS facilitates the development of mastitis by reducing host anti-inflammatory enzyme activity. In this study, we found that mastitis cows had distinct ruminal microbiota compositions and increased systemic inflammation, along with reduced host serum ALP levels. Reduced serum ALP was correlated with increased LPS levels in cows. RMT from mastitis cows (M-RMT) to recipient mice transferred mastitis symptoms through the LPS-mediated TLR4-cGAS-STING-NF- $\kappa$ B/NLRP3 pathways. Moreover, we showed that low-grade LPS exposure induced mastitis through reducing host ALP activity by the TLR4-neuraminidase (Neu)-ALP pathway, which further deteriorated *E. coli*-induced mastitis, as evidenced by supplementation with calf intestine alkaline phosphatase (cIAP) or the Neu inhibitor zanamivir, thus alleviating mastitis caused by low-grade LPS or *E. coli*. Our results highlight the important role of ruminal dysbiosis-derived low-grade endotoxemia in mastitis pathogenesis and act as a basis for the intervention of gut dysbiosis-associated extraintestinal diseases by restoring host anti-inflammatory enzyme levels.

## Materials and methods

### Experimental design

The experimental design has been shown in Fig. 1. We first investigated the ruminal microbiota profiles in



healthy and mastitis cows (Fig. 1A). To indicate the role of the ruminal microbiota in mastitis pathogenesis, RMT from healthy (H-RMT) and mastitis cows (M-RMT) to mice was performed (Fig. 1B). According to the differences identified between the healthy and mastitis groups in cows and RMT mice, we next investigated the role of ruminal dysbiosis-derived low-grade endotoxemia in the pathogenesis of mastitis in mice (Fig. 1C). Finally, we studied whether impaired host anti-inflammatory enzyme by ruminal dysbiosis aggravates pathogen-induced mastitis in mice (Fig. 1D).

**Collection of dairy cow samples**

Mastitis was diagnosed according to macroscopical inflammatory changes (e.g., redness, edema, fever, and pain) and somatic cell counts (SCC,  $SCC > 5 \times 10^5$  cells/mL) [33]. Healthy cows were defined as no mammary

injury and SCC less than  $2 \times 10^5$  cells/mL [34]. A total of 16 cows (4–6 years) were employed for the dairy sample collection, including 8 healthy and 8 mastitis cows from Qingzhou city, Shandong province, China. All cows were fed a standard diet consisting of hay and grains to meet their energy requirements [8, 33]. All healthy and mastitis cows were not exposed to antibiotics for 6 months before sample collection. The serum, milk, and ruminal samples were harvested aseptically and stored at  $-80^\circ\text{C}$  until determination of systemic inflammation, mastitis, and the ruminal microbiota, respectively.

**Animals and RMT treatment**

A total of 160 specific pathogen-free (SPF) grade BABL/c mice (22–24 g, 120 females and 40 males) were purchased from Liaoning Changsheng Biotechnology Co., Ltd. (Benxi, China). All mice were fed with sufficient standard

diet and water under SPF-grade feeding conditions with 12 h of light daily. The mice were further mated at a ratio of three females to one male until pregnancy was confirmed, and then the male mice were separated. The RMT model was established according to previously described methods [22, 23]. In brief, ruminal samples from each group, including the healthy and mastitis groups, were mixed and homogenized with sterile PBS at a final concentration of 50 mg/mL. The prepared homogenate was centrifuged at  $100\times g$  and 4 °C for 2 min, and then the supernatant was collected and dispensed based on experimental demand. Mice were transplanted 1 week after pregnancy. These mice were treated with antibiotic (200 mg/kg of ampicillin (Sigma Aldrich, USA), metronidazole (Sigma Aldrich, USA), and neomycin (Sigma Aldrich, USA) and 100 mg/kg vancomycin (Sigma Aldrich, USA)) daily through oral gavage for 5 days to eliminate commensal microbiota. Next, antibiotics were removed for 1 day, and mice were incubated daily with 300  $\mu$ L/mouse ruminal microbiota for three consecutive days and then twice a week for 3 weeks.

#### Low-grade LPS, cIAP, and zanamivir treatment

To investigate the role of low-grade LPS on the development of mastitis, mice were treated with LPS (2  $\mu$ g/mouse or 20  $\mu$ g/mouse daily,  $n = 5$ /group, *E. coli* 0111:B4, Sigma Aldrich, USA) intraperitoneally for 10 consecutive days from the first day of delivery according to previous studies [24, 32]. For treatment with cIAP and zanamivir, cIAP (20 U/mL,  $n = 6$ /group, Biolegend, CA, USA) or zanamivir (0.5 mg/mL,  $n = 6$ /group, Yuanyebio, Shanghai, China) was supplemented in the drinking water immediately following the initial LPS treatment and continued for the duration of the study as indicated [30].

#### Pathogen-induced mouse mastitis model

A mouse mastitis model was established by treatment with *E. coli* according to our previous description [20]. Briefly, *E. coli* were cultured in LB medium for 12 h to reach the mid-logarithmic phase. RMT-treated mice or conventional lactating mice 7 days after parturition were then separated from the offspring for three hours and injected with *E. coli* ( $10^7$  CFU/mL) through the milk ducts using a 100- $\mu$ L syringe with a 30-gauge blunt needle. To investigate the protective effects of host ALP on *E. coli*-induced mastitis in mice, lactating mice 7 days after parturition were pretreated with cIAP (75 U/kg, Biolegend, CA, USA) and zanamivir (500  $\mu$ g/kg, Yuanyebio, Shanghai, China) for 2 h followed by *E. coli* infection. Twenty-four hours after the *E. coli* injection, the mammary gland tissues were harvested and stored at  $-80$  °C until the detection of inflammatory parameters.

#### Histological analysis

All tissue samples used for histological analysis, including the mammary glands, ileum, colon, and liver tissues from RMT mice and the mammary glands from LPS- and *E. coli*-treated mice, were fixed with 4% paraformaldehyde for more than 48 h. The fixed samples were then embedded in paraffin and sliced into 5- $\mu$ m slices (five slices per mouse). The prepared sections were further stained with hematoxylin and eosin (H&E) and assessed with an optical microscope (Olympus, Tokyo, Japan). The histological score was determined as previously described [20].

#### Mammary cytokine detection

The mammary gland tissues from RMT-, LPS-, and *E. coli*-treated mice were weighed and homogenized (0.1 mg/mL) using PBS. The prepared homogenates were centrifuged at  $12,000\times g$  and 4 °C for 10 min, and the supernatants were collected for tumor necrosis factor (TNF)- $\alpha$  and interleukin (IL)-1 $\beta$  detection by using TNF- $\alpha$  and IL-1 $\beta$  ELISA kits (Biolegend, CA, USA).

#### Myeloperoxidase (MPO) activity determination

The mammary samples from RMT-, LPS-, and *E. coli*-treated mice were prepared to generate a 10% homogenate using the provided MPO buffer, and MPO activity was detected according to the manufacturer's instructions (Nanjing Jiancheng Bioengineering Institute, China).

#### Quantification of bacteria in the mammary glands of mice

To investigate the effects of different treatments on *E. coli*-induced mastitis, the mammary *E. coli* load was detected as previously described [35]. In brief, mammary samples were harvested aseptically and homogenized at a final concentration of 0.1 mg/mL using sterile PBS. The prepared homogenates were subjected to ten-fold serial dilutions until the desired concentrations were reached, and then the diluted homogenates were plated on MacConkey agar (Hopebio, Qindao, China). The number of *E. coli* was counted, and the absolute quantities were calculated based on the corresponding dilutions after 24 h of growth.

#### Serum LPS, ALP, and cytokine determination

Serum LPS levels from cows and RMT- and LPS-treated mice were detected as previously described [23]. In brief, the sera were collected under pyrogen-free conditions, and serum LPS levels were detected using a LPS ELISA kit according to the manufacturer's instructions (Lanpaibio, Shanghai, China). Serum ALP levels from cows and RMT-treated mice were measured

with an ALP assay kit according to the manufacturer's instructions (Nanjing Jiancheng Bioengineering Institute, China). Serum cytokines in cows and RMT-treated mice were detected using bovine TNF- $\alpha$  and IL-1 $\beta$  ELISA kits (Lanpaibio, Shanghai, China) and mouse TNF- $\alpha$  and IL-1 $\beta$  ELISA kits (Biolegend, CA, USA).

#### Test to determine pathogens in milk

To test for major mastitis pathogens, including *Staphylococcus aureus* (*S. aureus*), *Streptococcus*, and *E. coli*, in the milk of healthy and mastitis cows in this study, 50- $\mu$ L milk samples were plated on tryptone soya broth agar (TSB, Hopebio, Qindao, China), blood agar (Hopebio, Qindao, China), and MacConkey agar (Hopebio, Qindao, China), respectively. After 24 h of incubation, the numbers of bacterial colony-forming units (CFUs) were counted.

#### Routine blood tests and serum biochemical tests

A routine blood test was performed to detect the changes in blood immune cells in RMT-treated mice. Blood samples from RMT mice were collected into vacuum tubes with an anticoagulant (ethylenediamine tetraacetic acid), and then blood immune cells were detected with an automated hemocyte analyzer according to the manufacturer's instructions (HB-7510, Sinnova, China). Serum biochemical tests for cows and RMT-treated mice were performed as previously described [36]. Briefly, blood samples from cows and RMT-treated mice were collected into vacuum tubes with a coagulation activator (thrombin). Biochemical analysis was performed with an automatic analyzer (CS-T240, Dirui Industrial Co., Ltd., China) using the commercial veterinary kit (DiAvTest, Russia).

#### Lipocalin-2 assay

Fecal samples from the RMT treatment groups were weighed and prepared as 10% homogenates using PBS and then centrifuged at 3000 $\times$ *g* and 4 °C for 10 min. The supernatants were collected, and fecal lipocalin-2 levels were detected by ELISA according to the manufacturer's instructions (Lanpaibio, Shanghai, China).

#### Alcian blue (AB) staining

Paraffin sections of the colon were prepared as mentioned above. The prepared paraffin sections were dewaxed with xylene and serial alcohol solutions as previously described [28]. The sections were further stained using an Alcian Blue Stain Kit according to the manufacturer's instructions (Solarbio, Beijing, China).

#### Immunochemistry

All samples used for immunochemistry were prepared into 5- $\mu$ m sections and dewaxed as mentioned above, and immunochemistry was performed according to our previous study [20, 37]. Briefly, the dewaxed colon sections were subjected to antigen retrieval using sodium citrate and washed with PBS. The prepared sections were further incubated with endogenous peroxidase blockers (SAP (Mouse/Rabbit) IHC Kit, Maixin Biotechnology, Fuzhou, China) for 30 min and normal nonimmune goat serum (SAP (Mouse/Rabbit) IHC Kit, Maixin Biotechnology, Fuzhou, China) for 30 min at room temperature. The sections were further incubated with mucin-2 antibody (1:200, diluted with 5% goat serum, Affinity Biosciences, USA) overnight at 4 °C, and then the secondary antibody (goat-anti rabbit IgG) was added for 30 min of incubation at room temperature. Next, the sections were incubated with horseradish peroxidase (HRP) (SAP (Mouse/Rabbit) IHC Kit, Maixin Biotechnology, Fuzhou, China) for 20 min at room temperature and washed with PBS. After treatment with DAB color-developing fluid (Maixin Biotechnology, Fuzhou, China), the sections were stained with hematoxylin for 3 min and then differentiated with hydrochloric acid alcohol and ammonium hydroxide. After dehydration, the sections were sealed with neutral resin.

#### Total bacterial DNA extraction and Illumina NovaSeq sequencing

Ruminal samples from cows ( $n = 16$ , 8 cows from each group of the healthy and mastitis groups) and fecal samples from RMT-treated mice ( $n = 21$ , 7 mice from each of the control, H-RMT, and M-RMT groups) were used for bacterial DNA extraction and microbial analysis. Total genomic DNA from the ruminal and fecal samples was extracted using the CTAB method. DNA concentration and purity were monitored on 1% agarose gels. DNA was diluted to 1 ng/ $\mu$ L using sterile water. The 16S rRNA genes of the V4 region were amplified using a 515F-806R primer with the barcode. All PCRs were carried out with 15  $\mu$ L of Phusion<sup>®</sup> High-Fidelity PCR Master Mix (New England Biolabs), 2  $\mu$ M forward and reverse primers, and approximately 10 ng template of DNA. Thermal cycling consisted of initial denaturation at 98 °C for 1 min, followed by 30 cycles of denaturation at 98 °C for 10 s, annealing at 50 °C for 30 s, and elongation at 72 °C for 30 s. Finally, the samples were incubated at 72 °C for 5 min. The same volume of 1X loading buffer (containing SYB green) was mixed with the PCR products, and electrophoresis was performed on a 2% agarose gel for detection. Then, the PCR products were purified with a

Qiagen Gel Extraction Kit (Qiagen, Germany). Sequencing libraries were generated using the TruSeq<sup>®</sup> DNA PCR-Free Sample Preparation Kit (Illumina, USA) following the manufacturer's recommendations, and index codes were added. Library quality was assessed on a Qubit<sup>®</sup> 2.0 Fluorometer (Thermo Scientific) and Agilent Bioanalyzer 2100 system. Finally, the library was sequenced on an Illumina NovaSeq platform, and 250-bp paired-end reads were generated.

Alpha diversity was performed to analyze the complexity of taxa diversity, including observed species, Chao1, ace, and PD\_whole tree index. Principal coordinate analysis (PCoA) was performed to identify the microbial structures in the ruminal samples and fecal samples of the RMT mice. Linear discriminant analysis effect size (LEfSe) was performed to identify bacterial taxa that were differentially enriched in the different cows and RMT mice treatment groups [38]. Spearman correlation analysis was performed to analyze the relationship between different ruminal or gut microbial taxa and host parameters using Wekemo Bioincloud (<https://www.bioincloud.tech>). Tax4Fun analysis was performed to identify bacterial functions that were enriched in cows and RMT mice [39].

#### Total RNA extraction and quantitative RT-PCR

Total RNA was extracted from colonic tissues from RMT-treated mice ( $n = 7$  per group) using TRIzol (Invitrogen, Carlsbad, CA, USA), and quantitative RT-PCR was performed as described previously [20]. In brief, total RNA was extracted and prepared for cDNA. Furthermore, quantitative RT-PCR was performed using TransStart Tip Green qPCR SuperMix (TransGen Biotech, Beijing, China) and then FastStart Universal SYBR Green Master Mix (ROX) (Roche, Switzerland, Basel) in a Step One Plus apparatus (Applied Biosystems, Foster City, CA, USA). The  $2^{-\Delta\Delta C_t}$  method was utilized to determine the gene expression. GAPDH was used as an endogenous control, and all data were normalized to the control group. The primers used in this study are detailed in Additional file 1: Table S1.

#### Western blotting

Total protein extraction from mammary and colonic tissues and western blotting were performed according to previous studies [19, 20]. In brief, mammary and colonic samples were weighed and homogenized using tissue protein extract (Thermo Fisher Scientific, USA). After centrifugation at  $12,000\times g$  and  $4^\circ C$  for 10 min, the supernatants were harvested, and protein concentration determination was determined using a BCA Protein Assay Kit (Thermo Fisher Scientific, USA). SDS-PAGE (12% or 15%) was performed to separate the targeted

proteins according to molecular size. The targeted proteins were transferred to 0.45- $\mu m$  PVDF membranes and treated with 5% skim milk for 3 h at room temperature. Furthermore, specific primary antibodies, including p-p65, p-65, p-I $\kappa$ B, I $\kappa$ B, STING, p-TBK1, TBK1, p-IRF3, IRF3, occludin, ZO-1, and claudin-3 from Affinity Biosciences (OH, USA); TLR4, cGAS, NLRP3, ASC, and IL-1 $\beta$  from Cell Signaling Technology (Boston, USA); and  $\beta$ -actin from Immnoway Biotechnology (USA), were added for incubation at  $4^\circ C$  overnight. After incubating with secondary antibodies (goat anti-rabbit IgG or rabbit anti-mouse IgG, Immnoway Biotechnology, USA) for 2 h at room temperature, the proteins were detected using an ECL plus western blotting detection system.

#### Statistical analysis

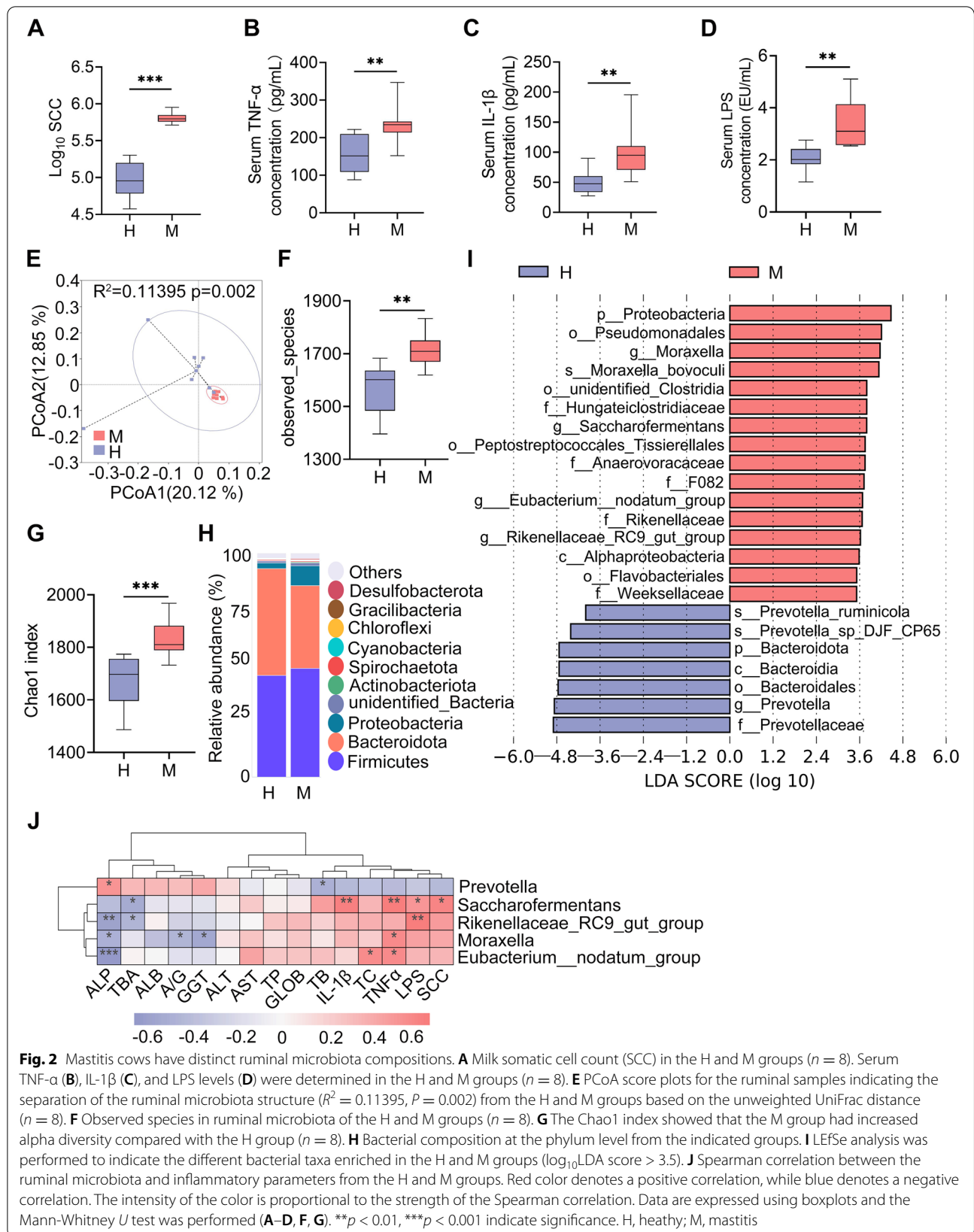
GraphPad Prism 8 (San Diego, CA, USA) was used for statistical analysis, and the data are expressed as the mean  $\pm$  SD or represented as a boxplot. Significant differences between the two groups were evaluated by the Mann-Whitney  $U$  test (nonparametric) or two-tailed unpaired Student's  $t$  test (parametric). For comparisons among more than two groups, a one-way analysis of variance (ANOVA) and a post hoc Tukey test were performed. For all statistical tests,  $p < 0.05$  indicates significance. Other specific statistical analyses are mentioned in the figure legends.

## Results

### Cows with mastitis have changed ruminal microbiota profiles and increased systemic inflammatory responses

To study the relevance between ruminal dysbiosis and mastitis in cows, 8 healthy cows (H) and 8 cows with clinical mastitis (M) were employed. Mastitis was diagnosed by increased milk SCC (Fig. 2A). Pathogen tests showed that mastitis cows had a higher load of *E. coli* in their mammary glands, but no significant differences in other pathogens were found (data not shown). We next performed serum biochemical tests and found that mastitis cows had changed liver function parameters and reduced serum ALP levels (Fig. S1). Furthermore, we confirmed that the M group had increased systemic inflammatory responses, as evidenced by increased contents of the serum proinflammatory cytokines TNF- $\alpha$  and IL-1 $\beta$  and LPS levels (Fig. 2B–D). These results indicated that mastitis cows had increased systemic inflammation.

We further investigated whether these increased systemic inflammation and mastitis parameters are related to the ruminal microbiota. Principal coordinate analysis (PCoA) showed a separation in the ruminal microbiota structure between the H and M groups based on unweighted UniFrac distance ( $R^2 = 0.11395$ ,  $p = 0.002$ , Fig. 2E). The M group had an increase in the observed



species in the ruminal microbiota compared with the H group (Fig. 2F). Other alpha diversity indices, including Chao1 (Fig. 2G), ace, and PD\_whole tree index were markedly increased in the M group compared with the H group (Fig. S2A–B). At the phylum level, *Proteobacteria* was enriched in the M group and *Bacteroidetes* was reduced (Fig. 2H). At the genus level, the ruminal microbiota composition between the H and M groups was significantly different (Fig. S2C). We further performed LEfSe analysis to identify the different bacterial taxa that were enriched in the H and M groups. The results showed that four bacterial genera, *Moraxella*, *Saccharofermentans*, *Eubacterium\_nodatum\_group*, and *Rikenellaceae\_RC9\_gut\_group*, were enriched in the M group compared with the H group (Fig. 2I). *Prevotella* was the only genus depleted in the M group compared with the H group (Fig. 2I). Furthermore, we showed that the M group had different bacterial functions compared with the H group (Fig. S2D–E). Tax4Fun analysis showed a marked separation of the metabolism pathways between the H and M groups with 26 pathways enriched in the M group, and 9 pathways were depleted (Fig. S2F). Several increases in potentially pathogenic bacterial pathways and aerobic respiration-associated pathways were detected in the M group, including nitrogen respiration, and plant and human pathogens (Fig. S2F). Additionally, the association between different key genera and systemic inflammatory parameters was determined by Spearman correlation analysis. The results showed that microbes enriched in the M group, including *Moraxella*, *Saccharofermentans*, *Eubacterium\_nodatum\_group*, and *Rikenellaceae\_RC9\_gut\_group*, were significantly positively correlated with most proinflammatory parameters and negatively correlated with serum ALP levels (Fig. 2J). In contrast, the correlation coefficient for *Prevotella* enriched in the H group was the opposite (Fig. 2J). These results suggest that cows with mastitis had distinct ruminal microbiota compositions and functions, which are associated with systemic inflammation and mastitis.

#### RMT from cows with mastitis (M-RMT) to mice induces mastitis in mice through the TLR4-cGAS-STING-NF- $\kappa$ B/NLRP3 pathways

To investigate the causative relationship between ruminal dysbiosis and mastitis, RMT from healthy (H-RMT) and mastitis cows (M-RMT) to recipient mice was performed (Fig. 3A). After 26 days of colonization, we found that M-RMT mice had significant mammary damage compared with that of control or H-RMT mice (Fig. 3B, C). To confirm this observation, we next showed that M-RMT increased the production of the proinflammatory cytokines TNF- $\alpha$  and IL-1 $\beta$  in the mammary gland compared with that of the control and H-RMT groups

(Fig. 3D, E). In addition, increased MPO activity, a specific marker for neutrophils, was detected in M-RMT mice compared with control or H-FMT mice (Fig. 3F). Moreover, M-RMT impaired the blood-milk barrier by reducing the tight junction (TJ) proteins ZO-1, occludin, and claudin-3 compared with the control and H-RMT groups (Fig. 3G, H). Of note, no significant differences were observed between control and H-FMT mice (Fig. 3A–H), which indicates that ruminal dysbiosis can induce mastitis symptoms in mice.

An increase in inflammatory cytokine production occurred due to the activation of proinflammatory pathways, such as NF- $\kappa$ B and NLRP3, which have been reported to play central roles in the pathogenesis of mastitis [19, 20]. Indeed, we found that M-RMT mice had higher NLRP3 and NF- $\kappa$ B activation than control or H-RMT mice by increasing NLRP3, ASC, IL-1 $\beta$ , p-p65, and p-I $\kappa$ B protein levels (Fig. 4A–G). Mounting evidence has recently shown that cyclic GMP-AMP synthase (cGAS)-mediated stimulator of interferon genes (STING) activation is a key regulator for the activation of the NF- $\kappa$ B and NLRP3 pathways [40–42], in which cGAS recognizes cytoplasmic DNA, such as mitochondrial DNA (mtDNA) caused by cellular stress or pathogen invasion to activate STING, leading to increased phosphorylation of TANK-binding kinase 1 (TBK1) and interferon regulatory factor 3 (IRF3) [42]. We next studied the expression of the cGAS-STING signature and showed that M-RMT mice had increased protein levels of cGAS, STING, p-TBK1, and p-IRF3 compared with those of control and H-FMT mice (Fig. 4H, J–M). Exposure to LPS has been reported to induce mtDNA synthesis through Toll-like receptor (TLR)-4 [42], which is also involved in the activation of the NF- $\kappa$ B and NLRP3 pathways and mastitis pathogenesis. As expected, we found that M-RMT increased the mammary TLR4 level compared with that of the control and H-FMT groups (Fig. 4H, I). These results suggest that the TLR4-cGAS-STING-NF- $\kappa$ B/NLRP3 pathways participate in M-RMT-induced mastitis in mice.

#### M-RMT induces a systemic immune imbalance and gut barrier leakage

We next investigated the effects of RMT on systemic and mucosal inflammation. We first determined the significant histological changes in the ileum, colon, and liver in the M-RMT group compared with the control and H-FMT groups (Fig. 5A, B). Consistently, M-FMT markedly increased the expression of the proinflammatory gene, including TNF- $\alpha$ , IL-1 $\beta$ , IL-6, and CCL2, in the colon compared with the control and H-RMT groups (Fig. 5C). In addition, we found that M-RMT increased the lipocalin-2 level, a marker of mucosal inflammation



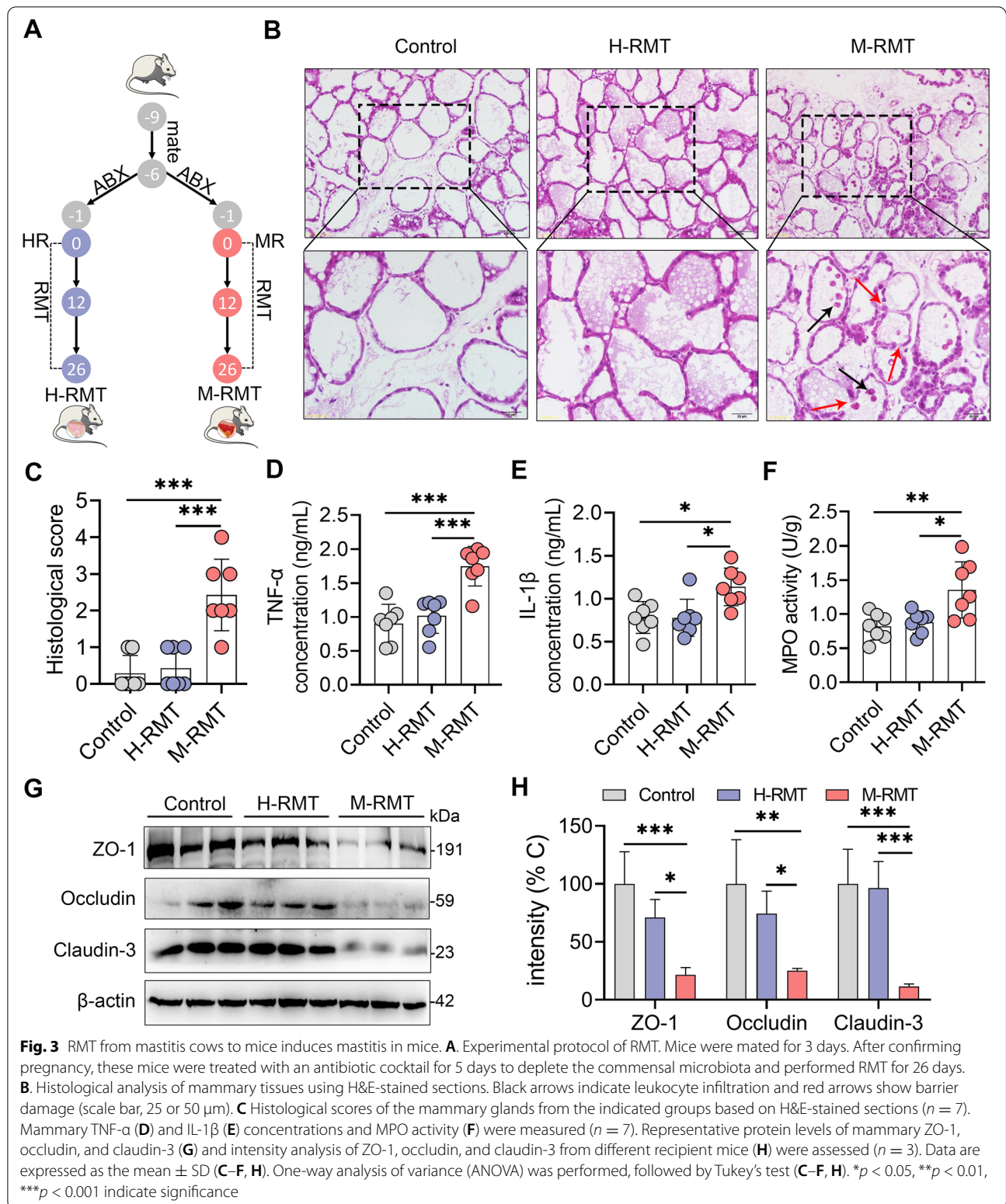
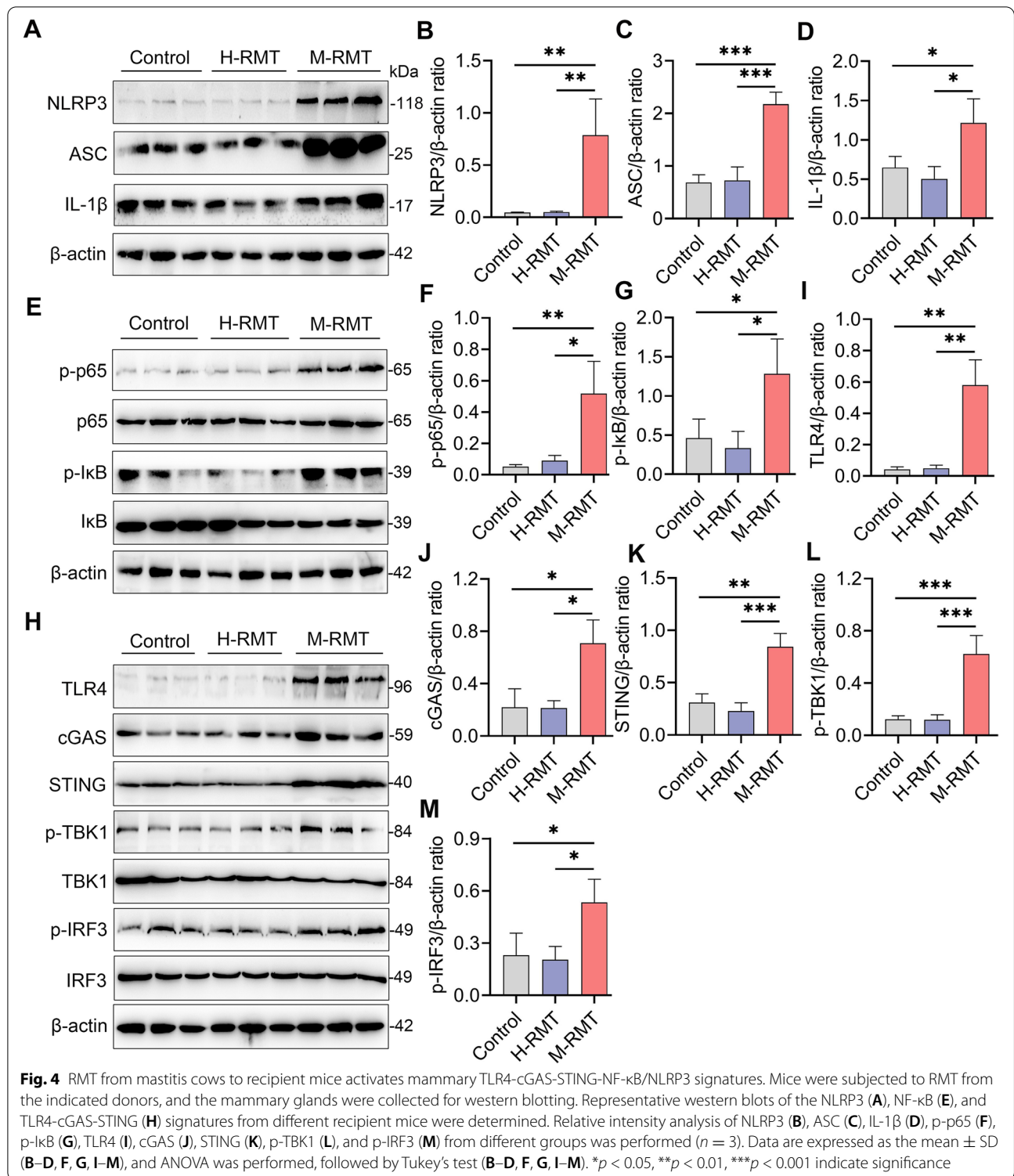


**Fig. 3** RMT from mastitis cows to mice induces mastitis in mice. **A**. Experimental protocol of RMT. Mice were mated for 3 days. After confirming pregnancy, these mice were treated with an antibiotic cocktail for 5 days to deplete the commensal microbiota and performed RMT for 26 days. **B**. Histological analysis of mammary tissues using H&E-stained sections. Black arrows indicate leukocyte infiltration and red arrows show barrier damage (scale bar, 25 or 50 μm). **C** Histological scores of the mammary glands from the indicated groups based on H&E-stained sections ( $n = 7$ ). Mammary TNF-α (**D**) and IL-1β (**E**) concentrations and MPO activity (**F**) were measured ( $n = 7$ ). Representative protein levels of mammary ZO-1, occludin, and claudin-3 (**G**) and intensity analysis of ZO-1, occludin, and claudin-3 from different recipient mice (**H**) were assessed ( $n = 3$ ). Data are expressed as the mean ± SD (**C–F, H**). One-way analysis of variance (ANOVA) was performed, followed by Tukey’s test (**C–F, H**). \* $p < 0.05$ , \*\* $p < 0.01$ , \*\*\* $p < 0.001$  indicate significance



[24], in the feces compared with those in control and H-RMT mice (Fig. 5D). We next showed that M-RMT, but not H-RMT, increased the monocyte and lymphocyte proportions in the blood (Fig. S3A), which was

accompanied by distinct serum biochemical characteristics (Fig. S3B). Moreover, we found that M-RMT mice had increased serum TNF-α and IL-1β levels compared with those in control and H-RMT mice (Fig. 5E, F). In

addition to these observations, M-RMT also increased serum LPS levels compared with the control and H-RMT groups (Fig. 5G). These results indicated that RMT from mastitis cows induced mucosal and systemic inflammation in mice.

Increased mucosal inflammation is known to destroy the gut barrier [23, 28], which orchestrates the first line of defense to protect the host against commensal or pathogenic microorganisms. We showed that M-RMT reduced the number of colonic goblet cells, which are responsible for the production of mucin [43], compared with the control and H-RMT groups (Fig. 5H). Consistently, M-RMT mice had decreased mucin-2 levels in the colon compared with control and H-RMT mice (Fig. 5H, I). Furthermore, we showed a significant decrease in the expression of genes related to TJs, such as *Tip1*, *occludin*, and *claudin-3*, in M-RMT mice compared with control and H-RMT mice (Fig. 5J). Likewise, M-RMT reduced ZO-1, occludin, and claudin-3 protein levels in the colon compared with the control and H-RMT groups (Fig. 5K, L). These data indicate that RMT from mastitis cows to recipient mice induced gut barrier disruption, resulting in endotoxemia and systemic immune balance.

#### M-RMT induces gut dysbiosis in recipient mice

We next investigated the changes in the gut microbiota of recipient mice. PCoA identified a marked separation in the gut microbiota compositions between the H-RMT and M-RMT groups based on the unweighted UniFrac distance ( $R^2 = 0.13452$ ,  $p = 0.025$ , Fig. 6A). Similar to the donor cows, mice in the M-RMT group had an increase in the observed species in the gut microbiota compared with those in the H-RMT group (Fig. 6B). Other alpha-diversity indices, including Chao1 (Fig. 6C), PD<sub>whole tree</sub> and ace index (Fig. S4A-B), were also markedly increased in the M-RMT group compared with the H-RMT group. At the phylum level, M-RMT increased *Proteobacteria* abundance and reduced *Bacteroidetes* abundance (Fig. 6D), which was similar to the differences between the H and M groups (Fig. 2H). Additionally, M-RMT reduced the abundance of *Firmicutes* in the gut microbiota of recipient mice (Fig. 6D). The difference in the microbiota composition between the H-RMT and M-RMT groups at the genus level was also significantly

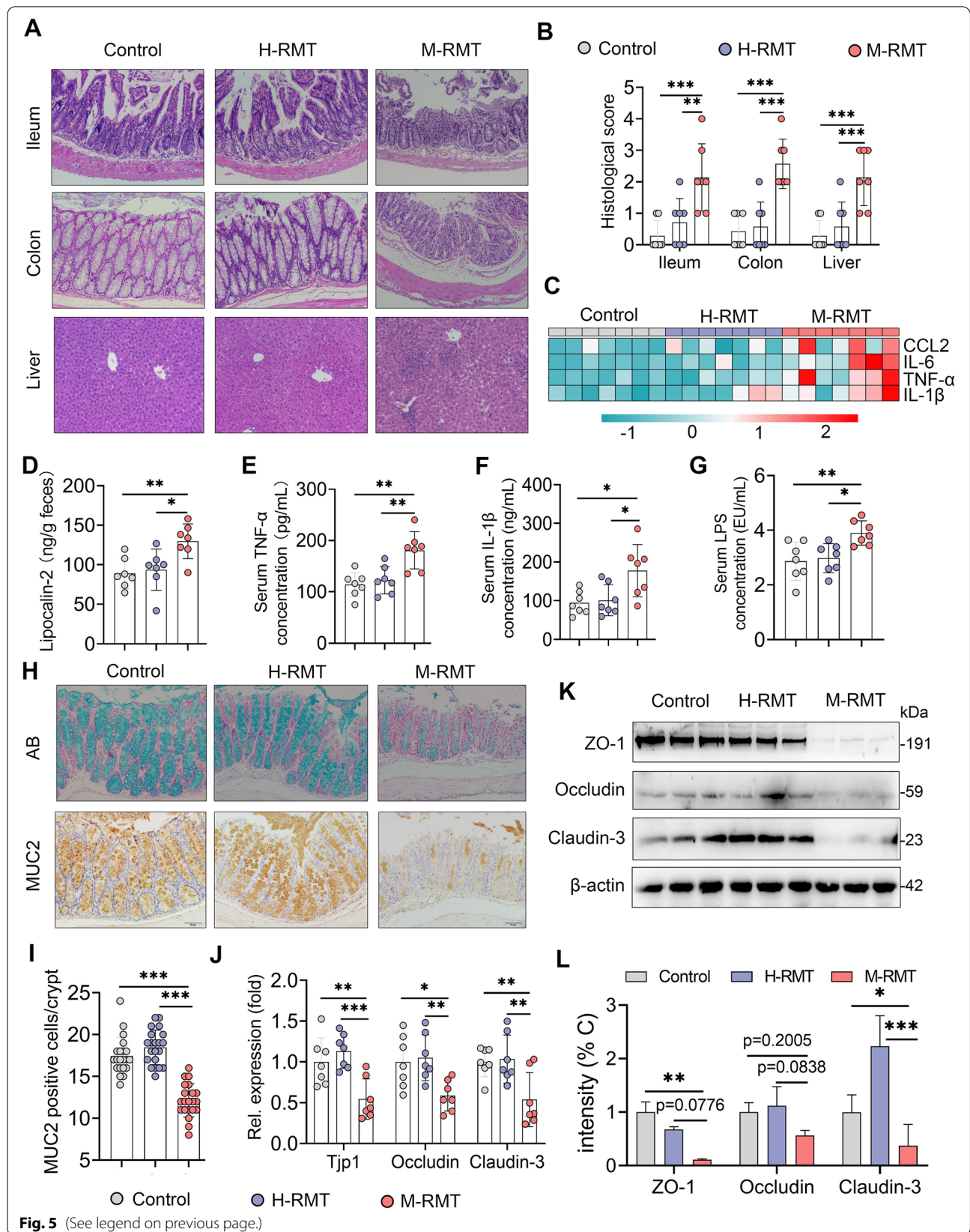
different (Fig. 6E). LEfSe showed that four bacterial genera, *Escherichia\_Shigella*, *Neisseria*, *Agathobacter*, and *Atopostipes*, were enriched in the M-RMT group compared with the H-RMT group (Fig. 6F), while *Ruminococcus\_gnavus\_group* was depleted in the M-RMT group compared with the H-RMT group (Fig. 6F). Consistent with the donor, we found that the M-RMT group had distinct bacterial functions compared with the H-RMT group, as 23 pathways were enriched in the M-RMT group, and 12 were depleted (Fig. S4C-E). Of note, the M-RMT group was enriched in several potentially pathogenic bacterial pathways and aerobic respiration-associated pathways that were also detected in the M group (Fig. S2F). Moreover, Spearman correlation analysis showed that microbes enriched in the M-RMT group, including *Escherichia\_Shigella*, *Neisseria*, *Agathobacter*, and *Atopostipes*, were significantly correlated with most of the proinflammatory parameters in the mammary gland, serum, and mucosa (Fig. 6G). These results indicate that M-RMT induced the differences in gut dysbiosis in recipient mice, which may be responsible for the development of systemic inflammation and mastitis.

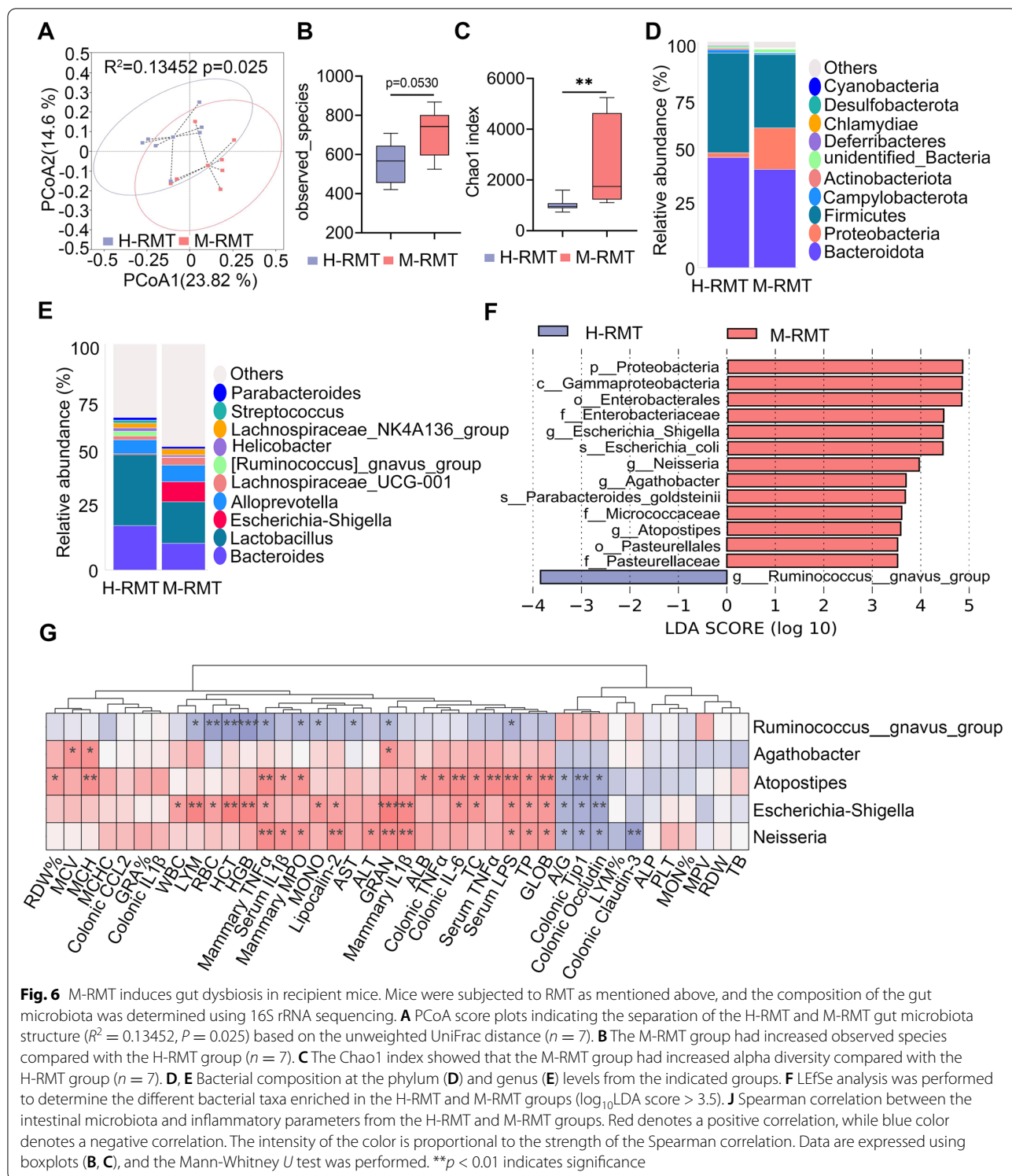
#### Recurrent exposure to low-grade LPS-induced mastitis in lactating mice

Considering the increase in serum LPS in the M group cows and M-RMT recipient mice, as well as the enriched gram-negative opportunistic pathogens, *Moraxella*, *Escherichia\_Shigella*, *Neisseria*, and *Agathobacter* in the M or M-RMT group, we then investigated the role of gut dysbiosis-derived low-grade endotoxemia in the pathogenesis of mastitis. Lactating mice were recurrently exposed to different doses of LPS intraperitoneally to mirror low-grade endotoxemia and serum LPS increased in a dose-dependent manner (Fig. 7A). Histological analysis showed that recurrent LPS exposure induced significant mammary injury compared with control mice (Fig. 7B, C). Consistently, recurrent LPS exposure increased the inflammatory marker levels, including mammary TNF- $\alpha$ , IL-1 $\beta$ , and MPO activity (Fig. 7D-F). In addition, recurrent exposure to LPS decreased the levels of the mammary TJ proteins ZO-1, occludin, and claudin-3 (Fig. 7G-J), indicating impaired blood-milk barrier integrity. Moreover, recurrent LPS exposure

(See figure on next page.)

**Fig. 5** M-RMT causes systemic immune imbalance and impairs the intestinal barrier in mice. **A** Representative ileum, colon, and liver H&E-stained sections from control, H-RMT, and M-RMT mice (scale bar, 50  $\mu$ m). **B** Histological scores of the ileum, colon, and liver from different treatment groups ( $n = 7$ ). **C** Proinflammatory gene expression in the colon was determined using qPCR ( $n = 7$ ). **D** Fecal lipocalin-2 levels from the indicated mice ( $n = 7$ ). Levels of serum TNF- $\alpha$  (**E**), IL-1 $\beta$  (**F**), and LPS (**G**) showed systemic inflammatory responses caused by M-RMT ( $n = 7$ ). The mucus layer of the colons from different recipient mice was examined by alcian blue (AB) staining (top, **H**), and immunohistochemistry was performed to assess the mucin-2 level in the colon using a mucin-2 antibody (bottom, **H**) (scale bar, 50  $\mu$ m). The positive-stained cells are shown in brown (**H**, **I**). **J** Relative mRNA levels of colon tight junction proteins, including *Tjp-1*, *occludin*, and *claudin-3*, from the indicated mice as determined by qPCR ( $n = 7$ ). **K**, **L** Protein levels of colon ZO-1, occludin, and claudin-3 were measured using western blotting ( $n = 3$ ). Data are expressed as the mean  $\pm$  SD (**B**, **D-G**, **I**, **J**, **L**), and one-way ANOVA was performed followed by Tukey's test (**B**, **D-G**, **I**, **J**, **L**). \* $p < 0.05$ , \*\* $p < 0.01$ , \*\*\* $p < 0.001$  indicate significance





activated the TLR4-cGAS-STING-NF- $\kappa$ B/NLRP3 pathways, as evidenced by increased TLR4, cGAS, STING, p-TBK1, p-IRF3, p-p65, p-I $\kappa$ B, NLRP3, ASC, and IL-1 $\beta$  contents, in a dose-dependent manner in the mammary

gland compared with the control group (Fig. 7G, K–T). These results suggest that gut dysbiosis-induced low-grade endotoxemia can trigger the development of mastitis in mice.

### Low-grade systemic endotoxemia facilitates mastitis through reducing ALP activity by the TLR4-neuraminidase (Neu)-ALP pathway

Single exposure to low-dose LPS was not enough to induce marked inflammatory responses, since the host had developed an orchestrated defense mechanism for LPS detoxification, such as ALP, which is widely distributed in the gut, liver, and mammary glands [30–32, 44]. Given the reduction in ALP in mastitis cows and M-RMT-recipient mice (Figs. S1 and S3B), we next investigated whether gut dysbiosis-derived low-grade systemic endotoxemia facilitates the development of mastitis by degrading ALP. We first showed that serum LPS levels were negatively correlated with serum ALP levels in cows and recipient mice (Fig. 8A, B). To confirm the role of ALP in protecting the host against systemic endotoxemia-induced mastitis, cIAP was applied during LPS treatment. Indeed, treatment with cIAP alleviated systemic endotoxemia-induced mammary injury and proinflammatory parameters compared with those in the LPS group (Fig. 8C–G). Additionally, treatment with cIAP improved the LPS-induced decrease in TJ proteins (Fig. 8H–K) and inhibited the activation of the TLR4-cGAS-STING-NF- $\kappa$ B/NLRP3 pathways caused by recurrent LPS exposure (Fig. 8H, L–R). These results suggest that host ALP reduction facilitates low-grade systemic endotoxemia-triggered mastitis in mice.

We next studied how gut dysbiosis-derived LPS reduces host ALP. TLR4-mediated sialylation through neuraminidase (Neu) has been shown to degrade ALP [30–32]. We therefore detected the gene expression of mammary *Neu1-4* in RMT recipient mice and found that M-RMT mice had increased *Neu3* levels in the mammary gland compared with control and H-RMT mice (Fig. 9A). Consistently, LPS treatment also increased *Neu3* level in the mammary gland compared with the control group (Fig. 9B). We therefore investigated the role of Neu3 in the development of mastitis by administering zanamivir, a specific Neu inhibitor [30, 32], to mice. The results showed that zanamivir treatment ameliorated systemic endotoxemia-induced mastitis (Fig. 9C–G). Additionally, zanamivir treatment restored the expression of TJ proteins and reduced the activation of the TLR4-cGAS-STING-NF- $\kappa$ B/NLRP3 pathways caused by recurrent

LPS exposure (Fig. 9H–R). These data indicate that low-grade systemic endotoxemia derived from gut dysbiosis can induce mastitis through the depletion of host anti-inflammatory ALP by the LPS-TLR4-Neu signature.

### Gut dysbiosis aggravates *E. coli*-induced mastitis in mice through ALP reduction by Neu activation

Considering the increased *E. coli* burden detected in mastitis cows in this study, we next studied whether this increase was attributed to gut dysbiosis. As expected, we found that *E. coli*-treated M-RMT mice developed more severe mastitis than *E. coli*-treated control and H-RMT mice (Fig. 10A, B). Similarly, *E. coli*-treated M-RMT mice had a higher *E. coli* burden in the mammary glands than *E. coli*-treated control and H-RMT mice (Fig. 10C). Given the protective role of ALP in recurrent LPS exposure-induced mastitis, we then studied whether a reduction in host ALP caused by increased Neu aggravates *E. coli*-induced mastitis. Indeed, treatment with ALP and zanamivir ameliorated *E. coli*-induced mastitis, as shown by improved mammary injury and reduced *E. coli* load in the mammary glands compared with the *E. coli* treatment group (Fig. 10D–F). Moreover, ALP and zanamivir reduced mammary proinflammatory markers caused by *E. coli* (Fig. 10G–I). These results suggest that gut dysbiosis aggravates *E. coli*-induced mastitis by reducing ALP via increasing Neu in mice.

## Discussion

Mastitis has been thought to be the most important factor influencing milk yield and quality, which not only causes great economic losses but also impairs animal health [45]. There is still a lack of an effective strategy for controlling mastitis based on interventions of local mammary inflammation and pathogen invasions, leading to other factors that participate in the development of mastitis. In the current study, we found that mastitis cows had higher systemic inflammatory parameters than healthy cows. Interestingly, cows with mastitis had reduced serum ALP levels that were negatively correlated with serum LPS concentrations. Using the RMT model, we further demonstrated that ruminal dysbiosis-derived low-grade endotoxemia contributes to mastitis by impairing host ALP activity and subsequently aggravates *E.*

(See figure on next page.)

**Fig. 7** Recurrent low-grade LPS exposure causes severe mastitis in lactating mice. Lactating mice were treated with LPS (2 or 20  $\mu$ g/mouse) intraperitoneally for 10 consecutive days after delivery, and then mammary tissues were harvested for determination. **A** Serum LPS levels from the indicated mice ( $n = 5$ ). **B** Representative mammary H&E-stained sections from differently treated mice (scale bar, 50  $\mu$ m). **C** Histological scores of the mammary glands from the indicated mice ( $n = 5$ ). **D, E** Mammary TNF- $\alpha$  (**D**), IL-1 $\beta$  (**E**), and MPO activities (**F**) in the different groups were determined ( $n = 5$ ). **G** Representative western blot images of tight junction and TLR4-cGAS-STING-NF- $\kappa$ B/NLRP3 pathway proteins in the mammary tissues from the indicated groups. The relative intensities of ZO-1, occludin, claudin-3, TLR4, cGAS, STING, p-TBK1, p-IRF3, p-p65, p-I $\kappa$ B, NLRP3, ASC, and IL-1 $\beta$  in the mammary glands (**H–T**) were determined ( $n = 3$ ). Data are expressed as the mean  $\pm$  SD (**A, C–F, H–T**), and one-way ANOVA was performed followed by Tukey's test (**A, C–F, H–T**). \* $p < 0.05$ , \*\* $p < 0.01$ , \*\*\* $p < 0.001$  indicate significance

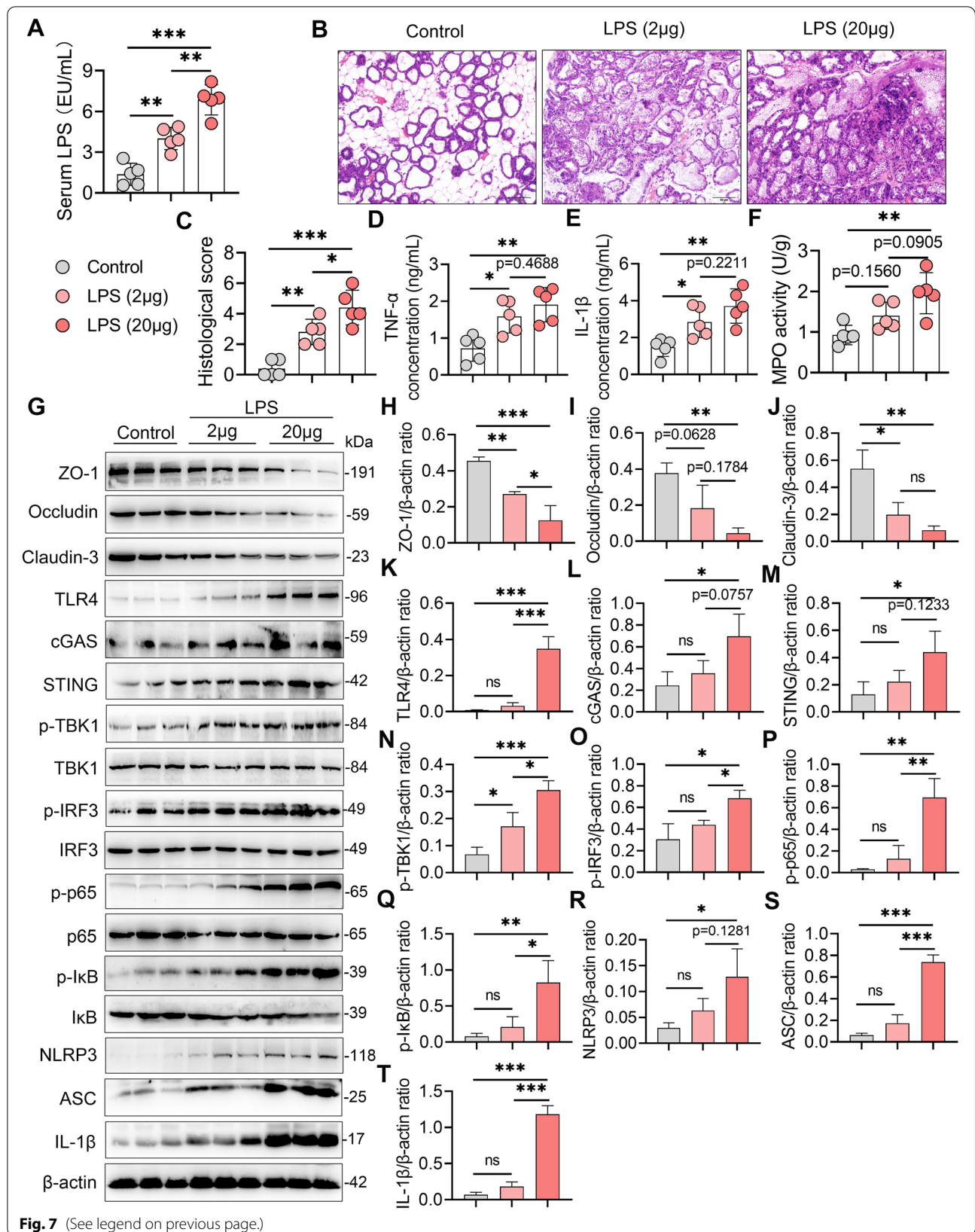


**Fig. 7** (See legend on previous page.)

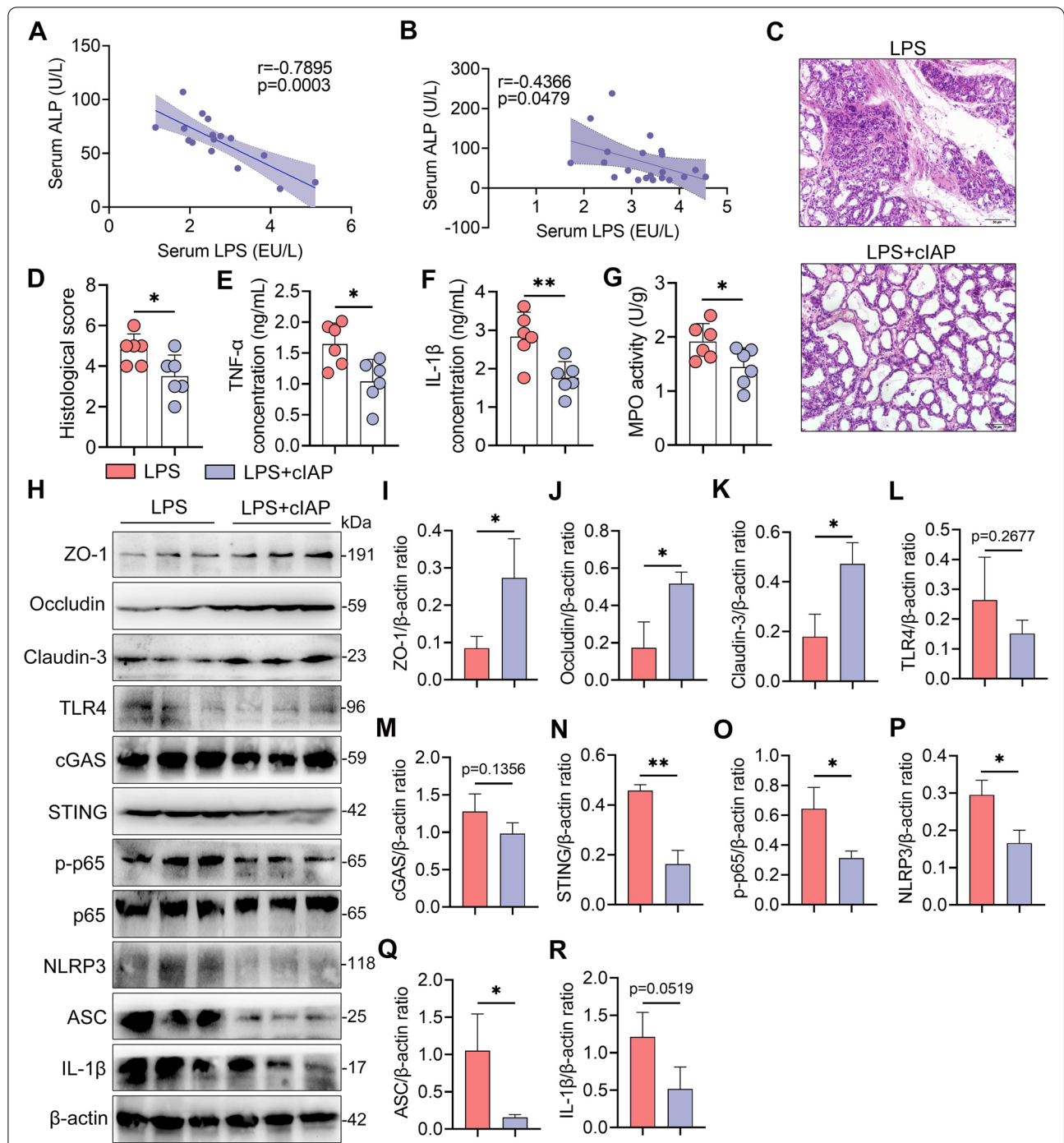


**Fig. 8** Gut dysbiosis-derived reduction in alkaline phosphatase (ALP) facilitates low-grade LPS exposure-induced mastitis in mice. **A, B** Correlation analysis showing that the serum LPS concentration is negatively correlated with serum the ALP level in cows (**A**) and mice (**B**). **C–G** Calf intestinal alkaline phosphatase (clAP) alleviates recurrent LPS exposure-induced mastitis ( $n = 6$ ). Mice were treated with or without clAP (20 U/mL) for 10 days during LPS treatment (20  $\mu$ g/mouse), and then the mammary glands were harvested. **C** Representative mammary H&E-stained sections from differently treated mice (scale bar, 50  $\mu$ m). **D** Histological scores of the mammary gland from the indicated mice. **E–G** Mammary TNF- $\alpha$  (**E**), IL-1 $\beta$  (**F**), and MPO activities (**G**) in the different groups were assessed ( $n = 6$ ). **H** Representative western blot images of tight junction and TLR4-cGAS-STING-NF- $\kappa$ B/NLRP3 pathway proteins in the mammary tissues from differently treated mice. **I–R** The relative intensities of ZO-1, occludin, claudin-3, TLR4, cGAS, STING, p-p65, NLRP3, ASC, and IL-1 $\beta$  in the mammary gland were determined ( $n = 3$ ). Data are expressed as the mean  $\pm$  SD (**D–G, I–R**), and one-way ANOVA was performed followed by Tukey's test (**D–G, I–R**). \* $p < 0.05$ , \*\* $p < 0.01$  indicate significance



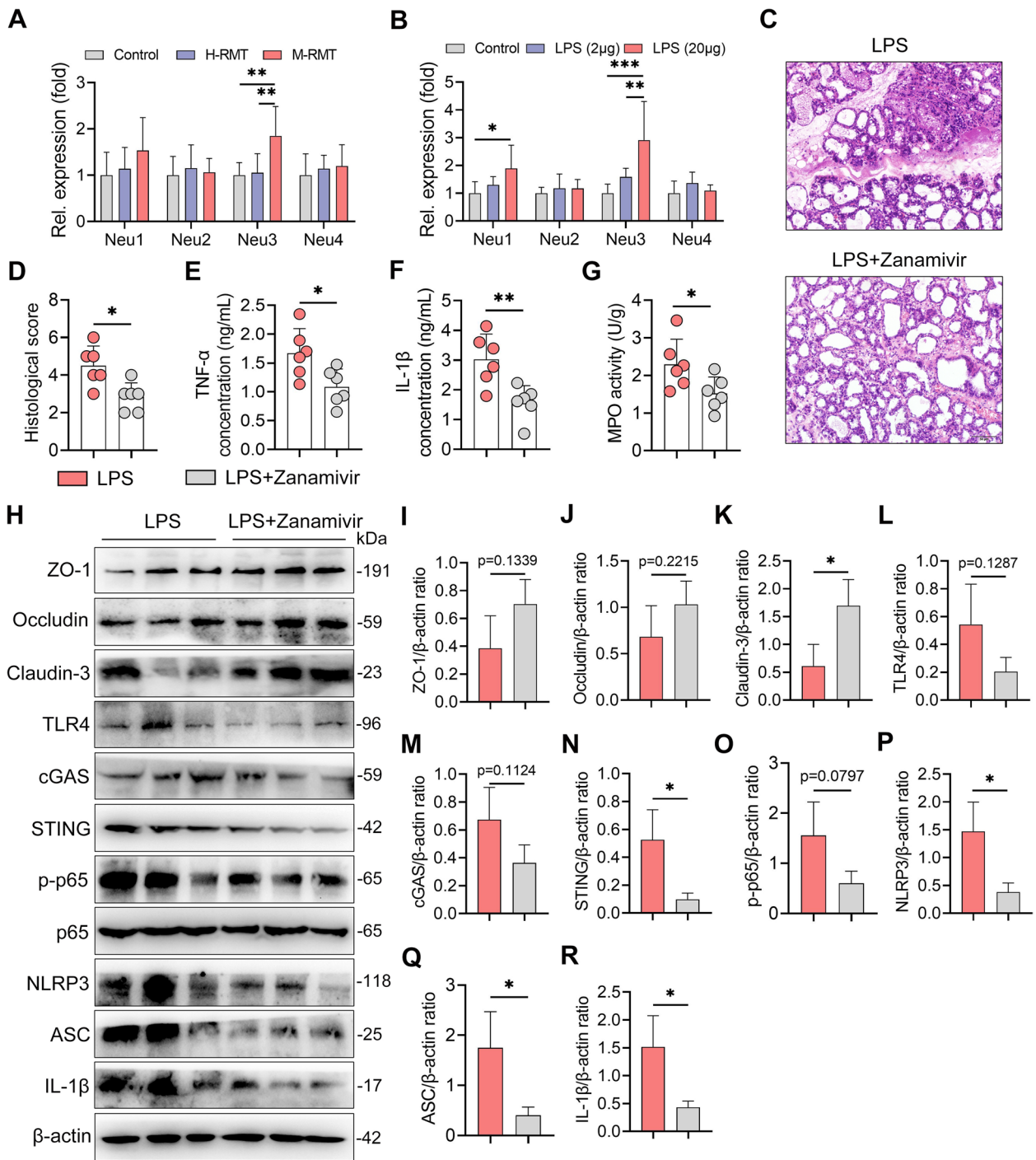


**Fig. 9** Gut dysbiosis-derived LPS reduces ALP by increasing neuraminidase (Neu3) in the mammary gland. **A, B** The relative gene expression of *Neu1-4* in RMT- (**A**) and LPS-treated mice (**B**) was detected using qPCR ( $n = 6$ ). **C–G** Neu inhibitor zanamivir improves recurrent LPS exposure-induced mastitis in mice. Mice were treated with or without zanamivir (0.5 mg/mL) for 10 days during LPS treatment (20 µg/mouse). **C** Representative mammary H&E-stained sections from differently treated mice (scale bar, 50 µm). **D** Histological scores of the mammary glands from the indicated mice ( $n = 6$ ). **E–G** Mammary TNF-α (**E**), IL-1β (**F**), and MPO activities (**G**) from different groups were assessed ( $n = 6$ ). **H** Representative western blot images of tight junction and TLR4-cGAS-STING-NF-κB/NLRP3 pathway proteins in the mammary tissues from differently treated mice. **I–R** The relative intensities of ZO-1, occludin, claudin-3, TLR4, cGAS, STING, p-p65, NLRP3, ASC, and IL-1β in the mammary glands were determined ( $n = 3$ ). Data are expressed as the mean ± SD (**D–G, I–R**), and one-way ANOVA was performed followed by Tukey’s test (**D–G, I–R**). \* $p < 0.05$ , \*\* $p < 0.01$  indicate significance

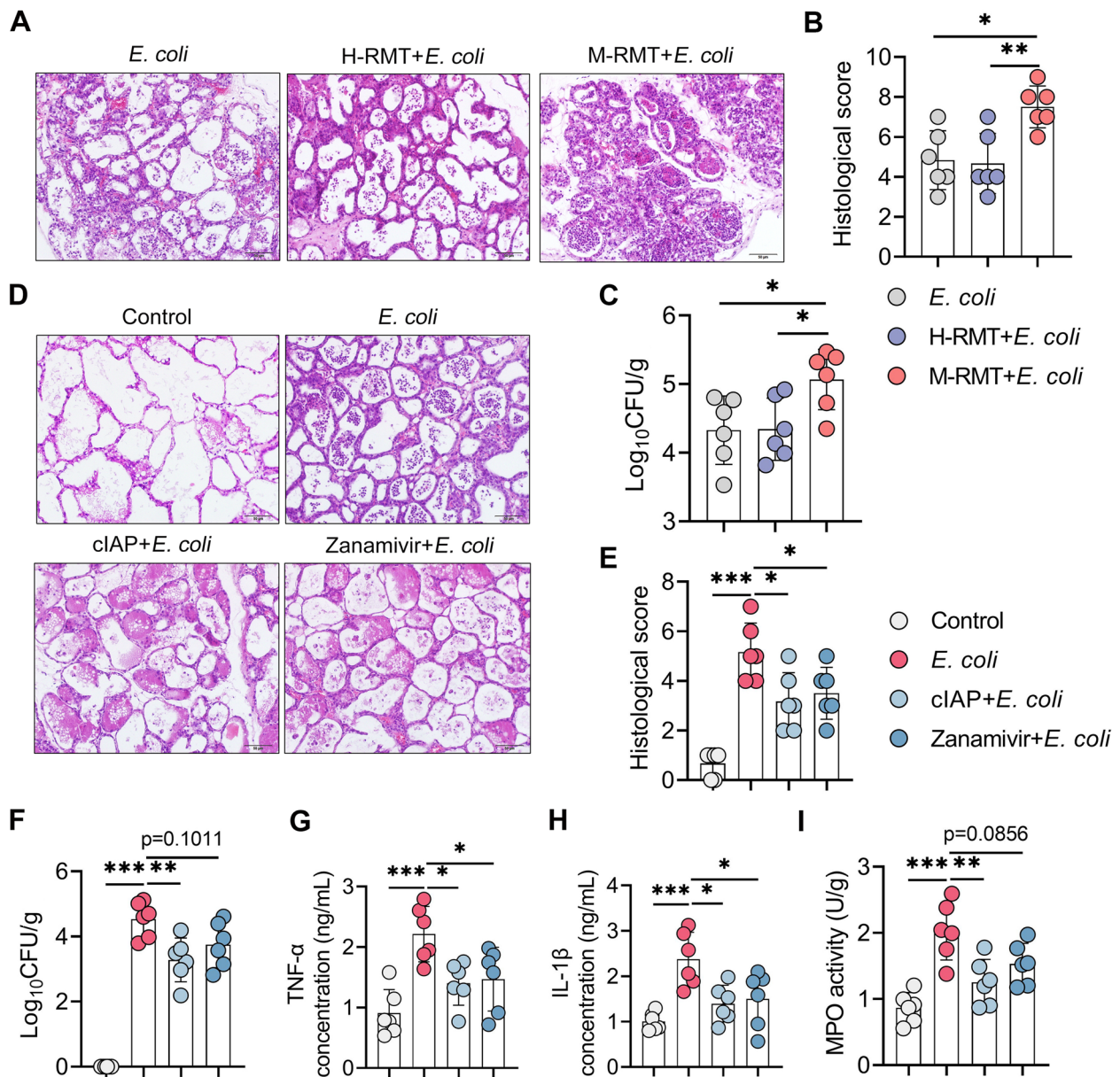


**Fig. 10** Gut dysbiosis aggravates *E. coli*-induced mastitis by reducing ALP. **A–C** M-RMT aggravates *E. coli*-induced mastitis in mice. Mice underwent RMT as mentioned above, and *E. coli* was administered to construct the mastitis model. **A, B** Representative H&E-stained mammary sections (**A**) (scale bar, 50 μm) and histological scores (**B**) ( $n = 6$ ). **C** Mammary *E. coli* detection showed that *E. coli*-treated M-RMT had a higher *E. coli* burden in the mammary gland ( $n = 6$ ). **D–I** Treatment with cIAP and zanamivir ameliorates *E. coli*-induced mastitis in mice. **D, E** Representative H&E-stained mammary sections (**D**) (scale bar, 50 μm) and histological scores (**E**) from differently treated mice ( $n = 6$ ). **F** Mammary *E. coli* loads in differently treated mice ( $n = 6$ ). Mammary TNF-α (**G**), IL-1β (**H**), and MPO (**I**) levels in the indicated groups were determined ( $n = 6$ ). Data are expressed as the mean ± SD (**B, C, E–I**) and one-way ANOVA was performed followed by Tukey’s test (**B, C, E–I**). \* $p < 0.05$ , \*\* $p < 0.01$ , \*\*\* $p < 0.001$  indicate significance. ns, no significance

*coli*-induced mastitis in mice. LPS has been used in many studies to establish mastitis models in mice and cows [46, 47]. Our results may thus extend the possibility that mammary LPS is derived from systemic circulation and

affected by other factors. Among the factors potentially involved in the pathogenesis is the ruminal microbiota, as evidenced by the increased occurrence of mastitis associated with ruminal dysbiosis [9, 10], such as SARA [8].

To investigate the association between mastitis and ruminal microbiota, healthy and clinical mastitis cows were employed for ruminal microbiota determination. As expected, mastitis individuals had distinct ruminal microbiota profiles, with especially enriched *Proteobacteria* and depleted *Bacteroidota*. Interestingly, *Moraxella*, *Saccharofermentans*, *Eubacterium\_nodatum\_group*, and *Rikenellaceae\_RC9\_gut\_group* were abundant, and *Prevotella* was reduced in the mastitis group compared with the healthy cows. *Moraxella* is known as a gram-negative pathobiont that causes inflammation, such as airway inflammation [48, 49]. We further showed that *Moraxella* was correlated with mastitis parameters, which agrees with a previous study showing that ruminal *Moraxella* abundance was changed in cows with mastitis [9]. *Saccharofermentans* has been reported to be enriched in HGD-induced ruminal dysbiosis and is related to increased serum amyloid A, C-reactive protein, haptoglobin, and lipopolysaccharide-binding protein [50]. Conversely, *Prevotella* has been thought to be a potential probiotic due to its capacity to produce propionate and was found to be depleted in the rumen of mastitis cows [9]. Likewise, these changed microbes were correlated with mastitis and systemic inflammatory markers. These results indicate that ruminal dysbiosis is associated with the development of mastitis and might be related to increased consumption of a HGD [8].

Transferring donor phenotypes to recipients is necessary to indicate the causation between microbiota changes and disease outcomes by using FMT and RMT [22, 33]. Although there are distinct differences in the physiological profiles and digestion systems between ruminants and non-ruminants, a previous study reported that the ruminal microbiota in cows is similar to the gut microbiota in the colon of mice by using RMT [22]. Notably, RMT from SARA cows with ruminal inflammation can induce colonic inflammation and endow similar microbial profiles in mice [22]. Likewise, FMT from mastitis cows to mice also induced mastitis in mice [33]. These findings indicate that mice are a good model to study mastitis in ruminants and that RMT may be a potential strategy that could be used to reveal the role of the ruminal microbiota in cow physiological functions and disease development. Indeed, we found that M-RMT, but not H-RMT, induced mastitis in recipient mice. Similar results were reported by a previous study in which FMT from cows with mastitis to mice induced mastitis [33], which supports the significant role of the microbiota in the gastrointestinal tract in the pathogenesis of mastitis. M-RMT damages the blood-milk barrier by reducing TJ expression, which is responsible for the exchange of substances between blood and milk and is often impaired during mastitis [19, 20]. Similar to

many gut dysbiosis-associated diseases [23, 24, 27, 51], M-RMT mice had increased mucosal inflammation and damaged intestinal barrier integrity, leading to increased serum LPS levels and systemic inflammation. Consistent with the donor cows, M-RMT mice had increased *Proteobacteria* and reduced *Bacteroidota*. At the genus level, *Escherichia\_Shigella*, *Neisseria*, *Agathobacter*, and *Atopostipes* were enriched in M-RMT mice. *Escherichia\_Shigella* and *Neisseria* are well-known gram-negative pathobionts correlated with intestinal inflammation [52–54] and mastitis [9, 20], which might account for the increase in serum LPS levels. Notably, increased LPS may probably facilitate ruminal and gut dysbiosis in turn [55].

Increased inflammatory cytokines are processed by host signaling transduction, such as NLRP3 and NF- $\kappa$ B, which have been widely proven to be involved in the pathogenesis of mastitis [20, 56]. As expected, M-RMT activated the NLRP3 and NF- $\kappa$ B pathways. Interestingly, the cGAS-STING signature has recently been reported to be the upstream regulator of NLRP3 and NF- $\kappa$ B [40–42, 57]. Our results were consistent with these findings, as evidenced by increased cGAS-STING and downstream p-TBK1 and p-IRF3 levels in mice in the M-RMT group. Moreover, M-RMT mice had increased TLR4 activation, which is consistent with increased serum LPS levels in the M-RMT group. Previous studies indicated that LPS can activate the cGAS-STING pathway through TLR4 [41, 42]. These results suggest the involvement of LPS-mediated TLR4-cGAS-STING-NF- $\kappa$ B/NLRP3 in the pathogenesis of ruminal microbiota-associated mastitis. Notably, our results did not allow us to rule out other receptor-mediated NLRP3 and NF- $\kappa$ B activation. Likewise, the increased cGAS-STING pathway may also be activated by microbial DNA derived from ruminal dysbiosis [58, 59].

The toxic form of LPS contains two phosphate groups coupled to glucosamines, and its recognition by TLR4 requires a full complement of typically six acyl chains in the lipid portion [60, 61]. The host has developed complex protective programs for LPS detoxification to avoid excessive immune activation. For example, host-produced acyloxyacyl hydrolase can remove secondary (acyloxyacyl-linked) fatty acids from LPS, rendering it immunologically inert [62, 63]. In addition, a single phosphate group removal by ALP is sufficient to generate a monophosphoryl lipid A, which is 100-fold less toxic than fully phosphorylated LPS [32, 64]. Detoxification of LPS may thus serve as an effective strategy to improve gram-negative bacteria-associated inflammation [30, 32]. Indeed, supplementation mice with cIAP alleviated recurrent LPS exposure-induced mastitis and inhibited the activation of inflammatory pathways. cIAP has also been reported to ameliorate recurrent *Salmonella*- or

*E. coli*-induced inflammation [30, 32]. In contrast to the ALP detoxification of LPS, consecutive LPS administration can in turn reduce ALP production by sialylation of ALP [30–32]. We found that both M-RMT and LPS exposure increased mammary Neu3 levels, which have been reported to prompt ALP degradation and are regulated by TLR4 [30–32]. Supplementing mice with the Neu inhibitor zanamivir alleviated recurrent LPS exposure-induced mastitis, which supports that diminished TLR4-mediated inflammation could be attributed to blocking host Neu [30–32]. These results suggest that ruminal dysbiosis or intestinal inflammation-derived low-grade LPS facilitates the development of mastitis by reducing host anti-inflammatory enzymes.

Apart from intestinal or systemic ALP production, ALP was also highly expressed in the mammary glands under homeostasis [44, 65], which indicates that reduced mammary ALP may facilitate gram-negative pathogen-induced mastitis. Indeed, M-RMT aggravated *E. coli*-induced mastitis compared with the control and H-RMT groups. In contrast, treatment with ALP or zanamivir alleviated *E. coli*-induced mastitis, which may explain why increased *E. coli* load was detected in mastitis cows in the current study. However, we did not exclude the role of other ruminal dysbiosis-derived factors in the increase in susceptibility to *E. coli* in the mammary gland. For example, ruminal dysbiosis-derived systemic inflammation endows damaged integrity of the blood-milk barrier and reduced abundance of commensal microbes induces host immune imbalance [8, 19, 20], which may lead to an increased possibility for pathogen invasion. In addition, studies have shown similar microbial profiles between the rumen or gut and the mammary gland during mammary diseases [8, 66, 67], which implies a potential pathogen transplantation across the gut-mammary axis. Future studies on these hypotheses will help to understand the pathogenesis of mastitis and seek new prevention and treatment strategies for mastitis.

## Conclusion

In summary, this study reveals that mastitis cows had marked ruminal microbiota disruption and increased systemic inflammation. Using the mouse RMT model, we showed that ruminal microbial dysbiosis contributes to the development of mastitis by inducing systemic inflammation and low-grade endotoxemia in mice. Low-grade endotoxemia impaired host ALP by activating Neu, causing persistent injury and mastitis by activating the TLR4-cGAS-STING-NF- $\kappa$ B/NLRP3 signatures. In addition, gut dysbiosis-derived ALP reduction aggravates *E. coli*-induced mastitis in mice. Our study for the first time demonstrates the effect of ruminal dysbiosis-derived low-grade endotoxemia in the development of mastitis,

which highlights the important role of the gut microbiota in the pathogenesis of mastitis and provides a potential strategy for the prevention of mastitis and other diseases by regulating the gut microbiota and host anti-inflammatory enzymes.

## Abbreviations

AB: Alcian blue; ALB: Albumin; ALT: Alanine aminotransferase; AST: Aspartate aminotransferase; ALP: Alkaline phosphatase; ANOVA: One-way analysis of variance; A/G: ALB/GLOB; cGAS: Cyclic GMP-AMP synthase; *E. coli*: *Escherichia coli*; FMT: Fecal microbiota transplantation; GLOB: Globulin; GGT:  $\gamma$ -Glutamyl transpeptidase; H-RMT: Ruminal microbiota transplantation from health cows; H: Health; H&E: Hematoxylin and eosin; IL-1 $\beta$ : Interleukin-1 $\beta$ ; IRF3: Interferon regulatory factor 3; LPS: Lipopolysaccharide; M: Mastitis; MPO: Myeloperoxidase; NF- $\kappa$ B: Nuclear factor- $\kappa$ -gene binding; NLRP3: NACHT LRR and PYD domains-containing protein 3; PCA: Principal components analysis; PCoA: Principal coordinate analysis; RMT: Ruminal microbiota transplantation; SD: Standard deviation; STING: Stimulator of interferon genes; *S. aureus*: *Staphylococcus aureus*; M-RMT: Ruminal microbiota transplantation from cows with mastitis; SPF: Specific pathogen-free; TB: Total bilirubin; TBA: Total bile acid; TBK1: TANK-binding kinase 1; TC: Total cholesterol; TJs: Tight junctions; TLR4: Toll-like receptor 4; TNF- $\alpha$ : Tumor necrosis factor- $\alpha$ ; TP: Total protein.

## Supplementary Information

The online version contains supplementary material available at <https://doi.org/10.1186/s40168-022-01402-z>.

**Additional file 1: Figure S1.** Serum biochemical characteristics in healthy and mastitis cows. Serum samples from healthy and mastitis cows were collected and performed for biochemical tests. Data were showed as heat map and \* $p < 0.05$  indicates significance by Student's t test. **Figure S2.** Mastitis cows have distinct ruminal microbiota structure and functions. A-B. Ace and PD\_whole\_tree index in the ruminal microbiota showed that cows with mastitis had increased alpha diversity. C. The bacterial composition at the genus level of the ruminal microbiota from healthy and mastitis cows. D. Top 10 bacterial functions of the ruminal microbiota in healthy and mastitis cows. E. PCA score plots for bacterial functions in the ruminal microbiota. F. Tax4Fun analysis shows top 35 bacterial functions in the ruminal microbiota in the indicated groups. Data are expressed as boxplots and \*\* $p < 0.01$  and \*\*\* $p < 0.001$  indicate significance by Mann-Whitney U test (A-B). **Figure S3.** Routine blood test and serum biochemical characteristics in RMT mice. **A.** Routine blood test from control, H-RMT and M-RMT mice showed that M-RMT mice had increased immune activation compared with that of control and H-RMT mice. **B.** Serum biochemical characteristics showed M-RMT mice had impaired liver function and reduced host ALP. **Figure S4.** RMT reshapes the gut microbiota structure and functions in recipient mice. A-B. PD\_whole\_tree and ace index in the gut microbiota showed that the M-RMT group had increased alpha diversity. C. The bacterial compositions at the genus level of the gut microbiota in the indicated mice. D. Top 10 bacterial functions of the gut microbiota in recipient mice. E. PCA score plots for bacterial functions in the gut microbiota. F. Top 35 bacterial functions in the gut microbiota in recipient mice by Tax4Fun analysis. Data are expressed as boxplots and \* $p < 0.05$  indicates significance by Mann-Whitney U test (A-B). **Table S1.** The oligonucleotides used in this study.

## Acknowledgements

We thank Zhaoqi He and Yuhong He from Zhang's Lab for their constructive suggestions for the study. The authors thank Xiaofei Zhou and Yue Ding from Animal Hospital, College of Veterinary Medicine, Jilin University, for their help with routine blood tests and serum biochemical tests.

## Authors' contributions

CZ, XH, YF, and NZ developed the hypothesis, designed all the experiments, and revised the manuscript. CZ, LB, KW, and YZ performed the major experiments. KX, SL, and YW performed the dairy sample collection. MQ, LF, and

XM participated in the animal treatments and cytokine and MPO activity measurements. LB performed the immunohistochemistry and part of western blotting. CZ wrote the main manuscript and performed the statistical analyses. All authors read and approved the final manuscript.

#### Funding

The study is supported by the National Natural Science Foundation of China (31972749, 32122087, and 32102738).

#### Availability of data and materials

All data generated during the current study are included in this article (and its supplementary information files). The 16S rRNA gene sequencing data in the present study are available in the NCBI Sequence Read Archive (SRA) repository under accession number PRJNA815921.

#### Declarations

#### Ethics approval and consent to participate

The animal experiments were approved by Jilin University (Changchun, China).

#### Consent for publication

Not applicable.

#### Competing interests

The authors declare that they have no competing interests.

#### Author details

<sup>1</sup>Department of Clinical Veterinary Medicine, College of Veterinary Medicine, Jilin University, Changchun 130062, Jilin Province, China. <sup>2</sup>Department of Breast Center, West China Hospital, Sichuan University, Chengdu 610041, Sichuan Province, China.

Received: 14 March 2022 Accepted: 24 October 2022

Published online: 01 December 2022

#### References

- Barbosa-Cesnik C, Schwartz K, Foxman B. Lactation mastitis. *JAMA*. 2003;289(13):1609–12.
- Puerto MA, Shepley E, Cue RI, Warner D, Dubuc J, et al. The hidden cost of disease: I. Impact of the first incidence of mastitis on production and economic indicators of primiparous dairy cows. *J Dairy Sci*. 2021;104(7):7932–43.
- He W, Ma S, Lei L, He J, Li X, et al. Prevalence, etiology, and economic impact of clinical mastitis on large dairy farms in China. *Vet Microbiol*. 2020;242:108570.
- Dalanezi FM, Joaquim SF, Guimarães FF, Guerra ST, Lopes BC, et al. Influence of pathogens causing clinical mastitis on reproductive variables of dairy cows. *J Dairy Sci*. 2020;103(4):3648–55.
- Jaeger S, Virchow F, Torgerson PR, Bischoff M, Biner B, et al. Test characteristics of milk amyloid A ELISA, somatic cell count, and bacteriological culture for detection of intramammary pathogens that cause subclinical mastitis. *J Dairy Sci*. 2017;100(9):7419–26.
- Peeler EJ, Green MJ, Fitzpatrick JL, Green LE. The association between quarter somatic-cell counts and clinical mastitis in three British dairy herds. *Prev Vet Med*. 2003;59(3):169–80.
- Pedersen RR, Krömker V, Bjarnsholt T, Dahl-Pedersen K, Buhl R, et al. Biofilm research in bovine mastitis. *Front Vet Sci*. 2021;8:656810.
- Hu X, Li S, Mu R, Guo J, Zhao C, et al. The rumen microbiota contributes to the development of mastitis in dairy cows. *Microbiol Spectr*. 2022;10(1):e0251221.
- Wang Y, Nan X, Zhao Y, Jiang L, Wang M, et al. Rumen microbiome structure and metabolites activity in dairy cows with clinical and subclinical mastitis. *J Anim Sci Biotechnol*. 2021;12(1):36.
- Chuang ST, Li KY, Tu PW, Ho ST, Hsu CC, et al. Investigating the reciprocal interrelationships among the ruminal microbiota, metabolome, and mastitis in early lactating Holstein dairy cows. *Animals*. 2021;11(11):3108.
- Alexander M, Turnbaugh PJ. Deconstructing mechanisms of diet-microbiome-immune interactions. *Immunity*. 2020;53(2):264–76.
- Stephen-Victor E, Crestani E, Chatila TA. Dietary and microbial determinants in food allergy. *Immunity*. 2020;53(2):277–89.
- Levy M, Kolodziejczyk AA, Thaïss CA, Elinav E. Dysbiosis and the immune system. *Nat Rev Immunol*. 2017;17(4):219–32.
- Torres J, Hu J, Seki A, Eisele C, Nair N, et al. Infants born to mothers with IBD present with altered gut microbiome that transfers abnormalities of the adaptive immune system to germ-free mice. *Gut*. 2020;69(1):42–51.
- Zhang T, Sun P, Geng Q, Fan H, Gong Y, et al. Disrupted spermatogenesis in a metabolic syndrome model: the role of vitamin A metabolism in the gut-testis axis. *Gut*. 2022;71(1):78–87.
- Cheng WY, Wu CY, Yu J. The role of gut microbiota in cancer treatment: friend or foe? *Gut*. 2020;69(10):1867–76.
- Vuong HE, Hsiao EY. Emerging roles for the gut microbiome in autism spectrum disorder. *Biol Psychiatry*. 2017;81(5):411–23.
- Thänert R, Thänert A, Ou J, Bajinting A, Burnham CD, et al. Antibiotic-driven intestinal dysbiosis in pediatric short bowel syndrome is associated with persistently altered microbiome functions and gut-derived bloodstream infections. *Gut Microbes*. 2021;13(1):1940792.
- Hu X, Guo J, Zhao C, Jiang P, Maimai T, et al. The gut microbiota contributes to the development of *Staphylococcus aureus*-induced mastitis in mice. *Isme J*. 2020;14(7):1897–910.
- Zhao C, Hu X, Bao L, Wu K, Feng L, et al. Aryl hydrocarbon receptor activation by *Lactobacillus reuteri* tryptophan metabolism alleviates *Escherichia coli*-induced mastitis in mice. *PLoS Pathog*. 2021;17(7):e1009774.
- Xie F, Jin W, Si H, Yuan Y, Tao Y, et al. An integrated gene catalog and over 10,000 metagenome-assembled genomes from the gastrointestinal microbiome of ruminants. *Microbiome*. 2021;9(1):137.
- Chen X, Su X, Li J, Yang Y, Wang P, et al. Real-time monitoring of ruminal microbiota reveals their roles in dairy goats during subacute ruminal acidosis. *NPJ Biofilms Microbiomes*. 2021;7(1):45.
- Chen X, Li P, Liu M, Zheng H, He Y, et al. Gut dysbiosis induces the development of pre-eclampsia through bacterial translocation. *Gut*. 2020;69(3):513–22.
- Carloni S, Bertocchi A, Mancinelli S, Bellini M, Erreni M, et al. Identification of a choroid plexus vascular barrier closing during intestinal inflammation. *Science*. 2021;374(6566):439–48.
- Lupp C, Robertson ML, Wickham ME, Sekirov I, Champion OL, et al. Host-mediated inflammation disrupts the intestinal microbiota and promotes the overgrowth of Enterobacteriaceae. *Cell Host Microbe*. 2007;2(2):119–29.
- Winter SE, Winter MG, Xavier MN, Thiennimitr P, Poon V, et al. Host-derived nitrate boosts growth of *E. coli* in the inflamed gut. *Science*. 2013;339(6120):708–11.
- Zhao Z, Ning J, Bao XQ, Shang M, Ma J, et al. Fecal microbiota transplantation protects rotenone-induced Parkinson's disease mice via suppressing inflammation mediated by the lipopolysaccharide-TLR4 signaling pathway through the microbiota-gut-brain axis. *Microbiome*. 2021;9(1):226.
- Shi H, Ge X, Ma X, Zheng M, Cui X, et al. A fiber-deprived diet causes cognitive impairment and hippocampal microglia-mediated synaptic loss through the gut microbiota and metabolites. *Microbiome*. 2021;9(1):223.
- Kang C, Wang B, Kaliannan K, Wang X, Lang H, et al. Gut microbiota mediates the protective effects of dietary capsaicin against chronic low-grade inflammation and associated obesity induced by high-fat diet. *mBio*. 2017;8(3):e00470–17.
- Yang WH, Heithoff DM, Aziz PV, Sperandio M, Nizet V, et al. Recurrent infection progressively disables host protection against intestinal inflammation. *Science*. 2017;358(6370):ea05610.
- Yang WH, Westman JS, Heithoff DM, Sperandio M, Cho JW, et al. Neu3 neuraminidase induction triggers intestinal inflammation and colitis in a model of recurrent human food-poisoning. *Proc Natl Acad Sci U S A*. 2021;118(29):e2100937118.
- Yang WH, Heithoff DM, Aziz PV, Haslund-Gourley B, Westman JS, et al. Accelerated aging and clearance of host anti-inflammatory enzymes by discrete pathogens fuels sepsis. *Cell Host Microbe*. 2018;24(4):500–513 e505.
- Ma C, Sun Z, Zeng B, Huang S, Zhao J, et al. Cow-to-mouse fecal transplantations suggest intestinal microbiome as one cause of mastitis. *Microbiome*. 2018;6(1):200.

34. Wittek T, Tichy A, Grassauer B, Egger-Danner C. Retrospective analysis of Austrian health recording data of antibiotic or nonantibiotic dry-off treatment on milk yield, somatic cell count, and frequency of mastitis in subsequent lactation. *J Dairy Sci.* 2018;101(2):1456–63.
35. Mwanyika G, Call DR, Rugumisa B, Luanda C, Murutu R, et al. Load and prevalence of antimicrobial-resistant *Escherichia coli* from fresh goat meat in Arusha, Tanzania. *J Food Prot.* 2016;79(9):1635–41.
36. Mironova I, Pleshkov A, Nigmatyanov A, Yarmukhamedova E, Islamova S. Efficiency of high-carbohydrate fodder in the diets of Holstein cows. *Vet World.* 2021;14(5):1303–10.
37. Zhao C, Bao L, Qiu M, Feng L, Chen L et al. Dietary tryptophan-mediated aryl hydrocarbon receptor activation by the gut microbiota alleviates *Escherichia coli*-induced endometritis in mice. *Microbiology spectrum.* 2022;10(4):e0081122.
38. Segata N, Izard J, Waldron L, Gevers D, Miropolsky L, et al. Metagenomic biomarker discovery and explanation. *Genome Biol.* 2011;12(6):R60.
39. Aßhauer KP, Wemheuer B, Daniel R, Meinicke P. Tax4Fun: predicting functional profiles from metagenomic 16S rRNA data. *Bioinformatics.* 2015;31(17):2882–4.
40. Wang W, Hu D, Wu C, Feng Y, Li A, et al. STING promotes NLRP3 localization in ER and facilitates NLRP3 deubiquitination to activate the inflammasome upon HSV-1 infection. *PLoS Pathog.* 2020;16(3):e1008335.
41. Li N, Zhou H, Wu H, Wu Q, Duan M, et al. STING-IRF3 contributes to lipopolysaccharide-induced cardiac dysfunction, inflammation, apoptosis and pyroptosis by activating NLRP3. *Redox Biol.* 2019;24:101215.
42. Ning L, Wei W, Wenyang J, Rui X, Qing G. Cytosolic DNA-STING-NLRP3 axis is involved in murine acute lung injury induced by lipopolysaccharide. *Clin Transl Med.* 2020;10(7):e228.
43. Desai MS, Seekatz AM, Koropatkin NM, Kamada N, Hickey CA, et al. A dietary fiber-deprived gut microbiota degrades the colonic mucus barrier and enhances pathogen susceptibility. *Cell.* 2016;167(5):1339–1353 e1321.
44. Folley SJ, Greenbaum AL. Changes in the arginase and alkaline phosphatase contents of the mammary gland and liver of the rat during pregnancy, lactation and mammary involution. *Biochem J.* 1947;41(2):261–9.
45. Hughes K, Watson CJ. The mammary microenvironment in mastitis in humans, dairy ruminants, rabbits and rodents: a One Health focus. *J Mammary Gland Biol Neoplasia.* 2018;23(1–2):27–41.
46. Gross JJ, Grossen-Rösti L, Wall SK, Wellnitz O, Bruckmaier RM. Metabolic status is associated with the recovery of milk somatic cell count and milk secretion after lipopolysaccharide-induced mastitis in dairy cows. *J Dairy Sci.* 2020;103(6):5604–15.
47. Kusebauch U, Hernández-Castellano LE, Bislev SL, Moritz RL, Røntved CM, et al. Selected reaction monitoring mass spectrometry of mastitis milk reveals pathogen-specific regulation of bovine host response proteins. *J Dairy Sci.* 2018;101(7):6532–41.
48. Padra M, Benktander J, Padra JT, Andersson A, Brundin B, et al. Mucin binding to *Moraxella catarrhalis* during airway inflammation is dependent on sialic acid. *Am J Respir Cell Mol Biol.* 2021;65(6):593–602.
49. Durack J, Huang YJ, Nariya S, Christian LS, Ansel KM, et al. Bacterial biogeography of adult airways in atopic asthma. *Microbiome.* 2018;6(1):104.
50. Chen H, Wang C, Huasai S, Chen A. Effects of dietary forage to concentrate ratio on nutrient digestibility, ruminal fermentation and rumen bacterial composition in Angus cows. *Sci Rep.* 2021;11(1):17023.
51. Shi H, Yu Y, Lin D, Zheng P, Zhang P, et al.  $\beta$ -Glucan attenuates cognitive impairment via the gut-brain axis in diet-induced obese mice. *Microbiome.* 2020;8(1):143.
52. Sovran B, Planchais J, Jegou S, Straube M, Lamas B, et al. Enterobacteriaceae are essential for the modulation of colitis severity by fungi. *Microbiome.* 2018;6(1):152.
53. Viladomiu M, Metz ML, Lima SF, Jin WB, Chou L, et al. Adherent-invasive *E. coli* metabolism of propanediol in Crohn's disease regulates phagocytes to drive intestinal inflammation. *Cell Host Microbe.* 2021;29(4):607–619.e608.
54. Wu F, Yang L, Hao Y, Zhou B, Hu J, et al. Oral and gastric microbiome in relation to gastric intestinal metaplasia. *Int J Cancer.* 2022;150(6):928–40.
55. Dai X, Hackmann TJ, Lobo RR, Faciola AP. Lipopolysaccharide stimulates the growth of bacteria that contribute to ruminal acidosis. *Appl Environ Microbiol.* 2020;86(4):e02193–19.
56. Qu S, Wang W, Li D, Li S, Zhang L, et al. Mangiferin inhibits mastitis induced by LPS via suppressing NF- $\kappa$ B and NLRP3 signaling pathways. *Int Immunopharmacol.* 2017;43:85–90.
57. Decout A, Katz JD, Venkatraman S, Ablasser A. The cGAS-STING pathway as a therapeutic target in inflammatory diseases. *Nat Rev Immunol.* 2021;21(9):548–69.
58. Luo Z, Ji Y, Gao H, Gomes Dos Reis FC, Bandyopadhyay G, et al. CRlg(+) macrophages prevent gut microbial DNA-containing extracellular vesicle-induced tissue inflammation and insulin resistance. *Gastroenterology.* 2021;160(3):863–74.
59. Erttmann SF, Swacha P, Aung KM, Brindefalk B, Jiang H, et al. The gut microbiota prime systemic antiviral immunity via the cGAS-STING-IFN-I axis. *Immunity.* 2022;55(5):847–861.e810.
60. Park BS, Song DH, Kim HM, Choi BS, Lee H, et al. The structural basis of lipopolysaccharide recognition by the TLR4-MD-2 complex. *Nature.* 2009;458(7242):1191–5.
61. Okuda S, Sherman DJ, Silhavy TJ, Ruiz N, Kahne D. Lipopolysaccharide transport and assembly at the outer membrane: the PEZ model. *Nat Rev Microbiol.* 2016;14(6):337–45.
62. Gorelik A, Illes K, Nagar B. Crystal structure of the mammalian lipopolysaccharide detoxifier. *Proc Natl Acad Sci U S A.* 2018;115(5):E896–e905.
63. Shao B, Lu M, Katz SC, Varley AW, Hardwick J, et al. A host lipase detoxifies bacterial lipopolysaccharides in the liver and spleen. *J Biol Chem.* 2007;282(18):13726–35.
64. Bentala H, Verweij WR, Huizinga-Van der Vlag A, van Loenen-Weemaes AM, Meijer DK, et al. Removal of phosphate from lipid A as a strategy to detoxify lipopolysaccharide. *Shock.* 2002;18(6):561–6.
65. Ali AT, Penny CB, Paiker JE, Psaras G, Ikram F, et al. The effect of alkaline phosphatase inhibitors on intracellular lipid accumulation in preadipocytes isolated from human mammary tissue. *Ann Clin Biochem.* 2006;43(Pt 3):207–13.
66. Soto-Pantoja DR, Gaber M, Arnone AA, Bronson SM, Cruz-Diaz N, et al. Diet alters entero-mammary signaling to regulate the breast microbiome and tumorigenesis. *Cancer Res.* 2021;81(14):3890–904.
67. Parida S, Wu S, Siddharth S, Wang G, Muniraj N, et al. A procarcinogenic colon microbe promotes breast tumorigenesis and metastatic progression and concomitantly activates Notch and beta-catenin axes. *Cancer Discov.* 2021;11(5):1138–57.

## Publisher's Note

Springer Nature remains neutral with regard to jurisdictional claims in published maps and institutional affiliations.

### Ready to submit your research? Choose BMC and benefit from:

- fast, convenient online submission
- thorough peer review by experienced researchers in your field
- rapid publication on acceptance
- support for research data, including large and complex data types
- gold Open Access which fosters wider collaboration and increased citations
- maximum visibility for your research: over 100M website views per year

At BMC, research is always in progress.

Learn more [biomedcentral.com/submissions](https://biomedcentral.com/submissions)

